Professor Lidia Morawska
International Laboratory for Air Quality and Health
Queensland University of Technology
2 George Street, Brisbane QLD 4001 Australia
Email: l.morawska@qut.edu.au

11th May 2017

Natascha Töpfer
Copernicus Publications
Editorial Support
editorial@copernicus.org

Dear Natascha,

Submission of Revised Manuscript Number: acp-2017-156

Title: Observations of Particles at their Formation Sizes in Beijing, China

Authors (names and email addresses):

Dr. Rohan Jayaratne: r.jayaratne@qut.edu.au
Ms. Buddhi Pushpawela: buddhi.pushpawela@hdr.qut.edu.au
Dr. Congrong He: c.he@qut.edu.au
Dr. Jian Gao: gaojian@craes.org.cn
Ms Hui Li: huili@craes.org.cn
Prof. Lidia Morawska: l.morawska@qut.edu.au

As requested, we have considered the comments of the two anonymous reviewers in detail and revised the paper accordingly.

I am submitting the following documents:

(1) Revised Manuscript

(2) Revised Manuscript with all changes indicated in Track Changes

(3) Detailed responses to Anonymous Reviewer 1 and

(4) Detailed responses to Anonymous Reviewer 2.

I hope you will find it acceptable for publication in ACP.

There are a few matters that I would like to bring to your notice for consideration:

1. We would like “Rohan Jayaratne” and “Buddhi Pushpawela” to be listed as Joint First Authors of this paper. We do understand that only the first name will be listed on the system.

2. If possible, we would like to add one more co-author: Fahe Chai. His contact details are as follows: Chinese Research Academy of Environmental Sciences, Beijing 100012, China. Email: chaifahe@craes.org.cn
3. If possible, we would like to add Jian Gao as a co-corresponding author of this paper. His contact details are as follows: Chinese Research Academy of Environmental Sciences, Beijing 100012, China. Email: gaojian@craes.org.cn
4. Referring to "Other Comment 1" by Anon Reviewer 2, we are aware that Prof Kulmala's name has been mis-spelt in the journal paper Kulmama et al (2016) FESE. Correcting this in our paper would deny their paper of a citation. We leave this to your discretion and would be happy to accept your decision.

Thank you.

Please contact me at the email address below, should you have any further queries.

Yours sincerely,

Professor Lidia Morawska, PhD

Director
International Laboratory for Air Quality and Health
WHO CC for Air Quality and Health

Director - Australia
Australia – China Centre for Air Quality Science and Management
Queensland University of Technology
Phone: +61 7 3138 2616
Fax: +61 7 3138 9079
E-mail: l.morawska@qut.edu.au

Interactive comment on "Observations of Particles at their Formation Sizes in Beijing, China" by Rohan Jayaratne et al.

Response to Comments from Anonymous Referee #1

Overall Comments

This paper contributes to the understanding of some of the factors that control new particle formation (NPF) events in more-polluted regions of the atmosphere. The paper is well written and falls within the scope of the journal. I find the comparisons between NPF and non-NPF days to be of particular interest, along with the detailed measurements of NPF events in the ~2-10 nm range by the NAIS, a range not well-captured by studies that rely on SMPS-type particle number concentration measurements alone. I recommend this paper to be published in ACP with minor revisions, as discussed below.

Response to Overall Comments

We thank the reviewer for these positive comments and are glad to note that the paper falls within the scope of the journal.

General comments:

Comment 1

Page 4, lines 81-83: This statement is confusing. Did the PNC exceed 10^5 cm^{-3} on all 45 days or just for the 25 days that NPF was observed? Please clarify.

Response 1

We accept that this sentence is confusing. We have amended it on page 4, lines 92-93 as follows:

"They observed NPF on 25 out of 45 days of measurement, and on each of these days the PNC exceeded 10^5 cm^{-3}."

Comment 2

Page 8, calculation of the diffusion coefficient: It would be good to include a brief discussion of the assumption that the main condensing vapor is sulfuric acid. Particle composition measurements were not a part of this work, but the authors do cite Yue et al. (2010) as showing that some NPF events in Beijing had sulfuric acid accounting for much less than half of the total growth rate, with organics accounting for ~55% of the growth. In the kinetic regime, the RMS speed of a molecule depends on 1/sqrt(MW), where MW = molecular weight = 98 g/mol for sulfuric acid = ~200 g/mol for organics. This would mean that organics would be about ~30% slower, and condensation in the kinetic regime is proportional to RMS speed. The continuum regime is trickier as it depends on the diffusion coefficient instead of

RMS speed, but if we simplify to assume everything is in the kinetic regime, then the CS would scale as sqrt(MW of sulfuric acid) / sqrt (MW of orgs) ~ sqrt(98) / sqrt(200). There are of course limited calculations and measurements of the diffusion coefficients of organic molecules as a function of temperature; however the authors could briefly comment on some of the literature values compared to their assumed value of D using sulfuric acid.

Response 2

In response to these comments, we have inserted the following text into the paper on page 8 and 9:

"It is now well established that sulfuric acid is the key precursor gas in nucleation, although low vapour pressure organics may contribute to the subsequent aerosol growth (Curtius, 2006). Sulfuric acid has a low vapour pressure which is reduced further in the presence of water. When produced from SO_2 in the gas phase, it is easily supersaturated and begins to condense. Moreover, most of the particles in the atmosphere are in the kinetic regime (smaller than 0.01 µm)(Seinfeld and Pandis, 2006). In this regime, condensation is directly proportional to the RMS speed of the molecules. The RMS speed is inversely proportional to the square root of the molecular weight of the molecule. Thus, a sulfuric acid molecule, with a molecular weight of 98 g mol^{-1}, has an RMS speed that is about 30% higher than a typical organic gas molecule with a molecular weight of about 200 g mol^{-1}, Thus, condensation of sulfuric acid will occur much more readily than organic molecules. Studies in Beijing have confirmed that NPF is more likely to occur in a sulfur-rich environment than in one that is sulfur-poor ((Yue et al., 2010;Guo et al., 2014;Wu et al., 2007)). Wu et al. (2007) also assumed that sulfuric acid was the main condensable vapour in determining the particle formation rates during NPF events in Beijing".

Our estimated values of D for sulfuric acid using the equation given in Jeong (2009) are 0.092 cm^2 s^{-1} at 303K and 0.087 cm^2 s^{-1} at 273K. The value of 0.092 cm^2 s^{-1} at 303K is reasonable as it is similar to other values given in the literature at room temperature, for example Brus et al. (2016) (0.08 cm^2 s^{-1}) and Eisele and Hanson (2000) (0.095 cm^2 s^{-1}).
The values of D for common organic trace gases as given in the literature are somewhat smaller than this, e.g. 0.07 cm^2 s^{-1} for isoprene (Tang et al., 2015) and terpenes (Williams, 2004). D for atmospheric amines are of the same order as that for sulfuric acid (Lugg, 1968)
Therefore, we feel that D = 0.092 cm^2 s^{-1} is a reasonable value to use in calculating the CS.

We have modified the text on page 10, lines 237-240 as follows:

"The mean temperature in Beijing during the period of observation was close to 0ºC. The value of D calculated using equation (2) at temperature T = 273 K was 0.087 cm2 s-1 which is in good agreement with the values given in the literature (Brus et al. (2016), Eisele and Hanson (2000)".

Comment 3

Page 9, condensation sink (CS) calculations: Why did the authors (1) choose to use 303 K in their diffusion coefficient (D) calculation (line 204) and (2) only use the SMPS PNC for the CS (line 203)? In regards to (1): temperature data wasn't reported in this paper but was taken as part of the meteorological data. The historical data reports Beijing's average temperature

in January as being around ~270 K. This difference in temperature doesn't lead to a particularly large change in D but certainly is worth addressing.

Response 3

3 (1) We accept the point about the temperature. The average temperature in Beijing during the observations was close to 273K. We have re-calculated our parameters using this value for T. The revised values are given below, and these have replaced the values in the paper.

3 (2) Regarding the point about calculating the CS, our response to this comment is included in Response 4 below.

Comment 4

In regards to (2): I would like to know why the authors chose to neglect the PNC data obtained from the NAIS for <14 nm size bins. A few calculations with "toy" size distributions show that, depending on the number concentration at these <14 nm bins, the CS can be non-trivially changed with the inclusion of these smaller bins. If the size distributions during NPF events in this paper such that the CS hardly changes with the inclusion of the smaller size bins, this should be stated.

Response 4

We have re-calculated the parameters, first by holding the temperature at 303K, in order to check if including the particles smaller than 14 nm will make a significant difference to the CS. We found that the CS value increased by about 8% (from 4.8 to 5.2 s^{-1}).

Therefore, we have re-calculated all the parameters using the value of CS obtained across the entire size range (< 14 nm from the NAIS plus >14 nm from the SMPS) and with the temperature changed from 303K to 273K.

The original values in the paper are as follows:

D = 0.092 cm^2 s^{-1}
CS = 4.8×10^{-3} s^{-1}
Coag = 8.3×10^{-4} s^{-1}
FR = 23 cm^{-3} s^{-1}

The new values obtained are as follows:

D = 0.087 cm^2 s^{-1}
CS = 4.2×10^{-3} s^{-1}
Coag = 7.2×10^{-4} s^{-1}
FR = 26 cm^{-3} s^{-1}

We have replaced all the values in the paper accordingly (Page 10, lines 237-240, Section 3.6, Section 3.7 and Table 3).

Comment 5

Page 13, lines 294-296: It is also worth mentioning that the pre-existing particles coming into the region from the winds from the south are also increasing the condensation sink, further reducing the likelihood of NPF.

Response 5

We have included the following text on page 13, lines 314-315:

"Pre-existing particles entering the region with the winds from the south will also increase the condensation sink, further reducing the likelihood of NPF."

Figures/Tables:

Comment 6

Each figure (excepting Fig 4) could benefit from being more professionally presented. I'm not sure what programming language was used to create these figures but if it is e.g. python, using savefig('name.png',dpi=300) and savefig('name.pdf') would create much nicer looking figures. The text is somewhat blurry and could benefit from being saved at a higher dpi (for png) or as a pdf without the grey backgrounds.

Response 6

Since first submission to ACP required embedding the figures within the body of the manuscript, the resolution of the figures has suffered. In the final submission, we shall present each figure as a separate file, so that they will be of much higher resolution.

For now, we have removed the grey background and the frames from all the figures.

Comment 7

Figures 2 and 7: The colorbars need labels of units. The numbers on the colorbars are quite blurry and need to be sharpened.

Response 7

The numbers that appear on the color bars are produced by the software. As we have provided two labels with the end point values, we feel that these intermediate numbers on the color bars are not essential. To compensate for this, we have further sharpened the text labels at the two ends of the color bars and have added the units (cm^{-3}).

Technical comments:

Comment 8

Abstract, lines 29-31: The sentence would read better is if said 'Estimated characteristics... are very different than to when the measurements. .

Response 8

The text has been changed as follows (Abstract, lines 30-32):

"Estimated characteristics of NPF events, such as their starting times and formation and growth rates of particles, are more accurate when the detection range of particles extends to smaller sizes".

Comment 9

Page 3, line 57: environments (needs an 's')

Response 9

The "s" has been added.

Comment 10

Page 11, line 247: no comma after 'that'.

Response 10

The comma has been deleted.

Comment 11

Page 16, line 385: This sentence might read better if it said '...in the smallest particle size bin 2-3 nm for the times at which the rate of increase. . .'

Response 11

We agree that the wording is unclear. The text has been changed on page 17, lines 416-418 as follows:

"...we calculated the formation rate of particles in the smallest particle size bin 2-3 nm. At these times, the rate of increase of particles in this size bin ranged from about 5.0×10^3 *to* 1.5×10^4 cm^{-3} h^{-1}*."*

References:

Brus, D., Skrabalova, L., Herrmann, E., Olenius, T., Travnickova, T., and Merikanto, J.: Temperature-dependent diffusion coefficient of H2SO4 in air: laboratory measurements using laminar flow technique, Atmos. Chem. Phys. Discuss., 2016, 1-26, 10.5194/acp-2016-398, 2016.
Curtius, J.: Nucleation of atmospheric aerosol particles, Comptes Rendus Physique, 7, 1027-1045, 2006.
Eisele, F., and Hanson, D.: First measurement of prenucleation molecular clusters, The Journal of Physical Chemistry A, 104, 830-836, 2000.
Guo, S., Hu, M., Zamora, M. L., Peng, J., Shang, D., Zheng, J., Du, Z., Wu, Z., Shao, M., and Zeng, L.: Elucidating severe urban haze formation in China, Proceedings of the National Academy of Sciences, 111, 17373-17378, 2014.
Jeong, K.: Condensation of water vapor and sulfuric acid in boiler flue gas, ProQuest, 2009.
Lugg, G.: Diffusion coefficients of some organic and other vapors in air, Analytical Chemistry, 40, 1072-1077, 1968.
Tang, M. J., Shiraiwa, M., Pöschl, U., Cox, R. A., and Kalberer, M.: Compilation and evaluation of gas phase diffusion coefficients of reactive trace gases in the atmosphere: Volume 2. Diffusivities of organic compounds, pressure-normalised mean free paths, and average Knudsen numbers for gas uptake calculations, Atmos. Chem. Phys., 15, 5585-5598, 10.5194/acp-15-5585-2015, 2015.
Williams, J.: Organic trace gases in the atmosphere: an overview, Environ. Chem., 1, 125-136, 2004.
Wu, Z., Hu, M., Liu, S., Wehner, B., Bauer, S., Wiedensohler, A., Petäjä, T., Dal Maso, M., and Kulmala, M.: New particle formation in Beijing, China: Statistical analysis of a 1-year data set, Journal of Geophysical Research: Atmospheres, 112, 2007.
Yue, D., Hu, M., Zhang, R., Wang, Z., Zheng, J., Wu, Z., Wiedensohler, A., He, L., Huang, X., and Zhu, T.: The roles of sulfuric acid in new particle formation and growth in the mega-city of Beijing, Atmospheric Chemistry and Physics, 10, 4953-4960, 2010.

Interactive comment on "Observations of Particles at their Formation Sizes in Beijing, China" by Rohan Jayaratne et al.

Response to Comments from Anonymous Referee #2

General comments:

For this paper, the authors employed a Neutral cluster and Air Ion Spectrometer (NAIS) to investigate the early steps of new-particle formation (NPF) events in Beijing, China, over a period of 3 months. Specifically, observations were made down to particle (or cluster) sizes of about 2nm. NPF events in large, polluted urban areas, in particular in E Asia, are a current subject of atmospheric research (e.g. Kulmala et al., 2017). To my knowledge, this is the first report on deploying an NAIS in a Chinese megacity for this purpose, and it constitutes one of recent attempts of improving on the observations of NPF in such environments by directly measuring in the sub-3 nm size range (cf. Cai and Jiang, 2017; Yu et al., 2016). As such, the study is timely and of interest to the scientific community engaged in this field, and I recommend its publication in Atmospheric Chemistry and Physics.

Response to General Comments

We thank the reviewer for these positive comments and are glad to note that he/she feels that the paper would be of interest to the scientific community engaged in this field, and for recommending that, subject to the changes below, it is suitable for publication in Atmospheric Chemistry and Physics.

Major Comments 1

Before that however, I recommend a major revision to take care of some important issues.

My main concern with the study in its present form is the treatment and discussion of the NAIS measurements for the sub-3 nm size range. The treatment, presentation and interpretation of these data need to be brought into a form more rigorously consistent within the paper itself, as well as with best-practices recommended by the community (Manninen et al., 2016) – in particular as the corresponding results are a major selling point here.

Comments regarding sub-3 nm measurements:
Lines 109-110: "The NAIS … can detect particles down to a size of 0.8 nm":
My main point is that the NAIS can actually *not* be used to measure *neutral* compounds down to this size, so this statement is misleading in its current form. The NAIS does detect ions with the corresponding mobility, but due to the interference from charger ions it is deemed not possible to determine concentrations of neutral clusters for the smallest size bins. Quoting Manninen et al. (2016), which is cited also in this paper (line 137), "the particles below about 2 nm cannot be reliably distinguished from the corona-generated ions. Typically, the lowest detection limit for the NAIS in the particle mode is between 2 and 3 nm depending on the corona voltage and on the properties and composition of carrier gas (environmental conditions)." Details can be found in their paper and references therein. At one occasion later, the authors appear to consider this instrumental limitation, e.g. section 2.2.3.

Response to Major Comments 1

We agree with these comments and accept that the NAIS has a problem in differentiating between charged and neutral particles and clusters at sizes below 2.0 nm owing to the presence of corona-generated ions as pointed out by Asmi et al. (2009), Manninen et al. (2011) and Manninen et al. (2016).

We have addressed this issue and made the following changes to the paper:

1. Considering the limitations of the NAIS in measuring total particle and cluster concentrations at sizes smaller than 2 nm, we have restricted our observations to particles that are larger than 2.0 nm.
2. This led to the smallest size bin (1.6-2.0 nm) being excluded from the particle analyses and we have replaced '1.6 nm' with '2.0 nm' at all relevant points in the text.
3. We estimated that this decreased our charged and neutral PNC values by about 5%. We have made this change right through the manuscript.
4. In Table 2, we have removed the two columns showing charged and neutral cluster concentrations.
5. In Figure 7, we have removed the three points below 2.0 nm and inserted a note in the caption cautioning against using the data below 2.0 nm.
6. Similarly, in Figure 2(a), we have inserted a note stating that the data below 2.0 nm should be treated with caution.

In addition, we have incorporated the following changes to the text:

Lines 109-110: we have replaced the text "can detect particles down to a size of 0.8 nm" with the following text on page 5 (New line numbers 119-120):

"The NAIS is specifically designed to monitor NPF as it can detect particles down to their actual formation sizes"

Line 136 - : We have inserted the following text on page 6 (New line numbers 146-152):

"However, Asmi et al. (2009), Manninen et al. (2011) and Manninen et al. (2016) have pointed out that the lowest detection limit for the NAIS in the particle mode is about 2.0 nm owing to the presence of corona-generated ions. Therefore, at sizes smaller than 2.0 nm, the NAIS cannot reliably distinguish between charged and neutral particles Therefore, Manninen et al. (2011) specified the lowest detection limit of the NAIS to be 1.6 and 1.7 nm for negative and positive ions, respectively, and 2.0 nm for neutral particles. Therefore, in this study, we will restrict our observations to the particle size range 2.0-42 nm."

Section 2.1.1 Line 165 - : we have amended the text as follows on section 2.3.1. (New line numbers 181-182):

"..where N is the number of particles in the size range 2.0 -10.0 nm."

While changing the definition of the lower end of N from 1.8 nm to 2.0 nm affected the total PNC in that size range by about 5%, it did not affect the decisions regarding the identification of any of the NPF events.

Line 170: The text has been changed to the following (Page 8, new line numbers 189-190):

"The starting times of an event was determined by using the time of sudden increase in total PNC in the size range 2.0 – 10.0 nm."

Line 223: The text has been changed to the following (Page 11, new line numbers 263-264):

"…we exported the number concentrations of particles obtained from the NAIS in 14 bins in the size range 2.0 – 42.0 nm."

Major Comments 2

Section 3.4 (including Fig. 5 and Table 2) discusses charged vs. neutral "cluster" and "particle" concentrations. Here, the authors need to state what is their definition of "cluster" and "particle". And in light of the above, they might need to reconsider if total neutral cluster concentrations (as implied in section 3.4) can even be derived from the NAIS measurements! The discussions throughout section 3.4 may have to be revised. E.g., depending on those definitions, could the observed decreases of "neutral clusters" for NPF days (e.g. Fig. 5b) be explained by instrument response to a change in environmental conditions?

Response to Major Comments 2

We have provided the conventional definitions of clusters and particles from the literature in our introduction. In Section 3.4, we have restricted our analysis to particles larger than 2.0 nm. This has resulted in the smallest size bin (1.6-2.0 nm) being excluded from the particle analyses. We estimated that this decreased our charged and neutral PNC values by about 5%. We have made this change right through the manuscript. The sub-heading title has been changed to "*Charged Particles*". All references to cluster concentrations have been removed. In Fig 5, we have removed Fig 5(b) that showed the neutral and charged cluster concentrations. Fig 5 now shows only the neutral and charged particle concentrations (larger than 2.0 nm).

In Table 2, we have removed the two columns showing charged and neutral cluster concentrations.

Major Comments 3

Figure 2, top panel, and Figure 7:
As a consequence, I would argue that particle size distribution data below 2 nm shouldn't even be shown. The concentrations at the size bins <2 nm are subject to instrumental factors, not necessarily resulting from actual variations in the concentrations of sub-2 nm neutral clusters (particles). Hence, their display here could prompt an unaware reader to draw wrong conclusions about the actual population of sub-2 nm neutral clusters.

Response to Major Comments 3

In Figure 7, we have excluded the three points below 2.0 nm and inserted a note in the caption cautioning against using the data below 2.0 nm.

Similarly, in the caption to Figure 2(a), we have inserted a note stating that the data below 2.0 nm should be treated with caution.

Other comments:

Comment 1

Line 68: Kulmama should probably be Kulmala – also in later instances for this reference.

Response 1

In the journal paper the name has been mis-spelt as 'Kulmama". Correcting this is bound to affect the citation count and we will seek the advice of the Editor on this matter and make the change, if required.

Comment 2

Speaking of which, the recent paper by Kulmala et al. (2017) is relevant to this study and should be brought to attention in the introduction. As condensation sinks were calculated for this study, it might be useful even to shortly discuss the authors' findings in light of the conclusions of that paper (see e.g. lines 237-239).

Response 2

We agree. We have inserted the following text into the Introduction (Page 3, lines 69-77):

"Kulmala et al (2017) proposed that the survival efficiency of clusters to form particles is determined by the two key parameters – condensation sink (CS) and cluster growth rate (GR). They defined a dimensionless survival parameter, P, equal to the ratio $(CS/10^{-4}\ s^{-1})/(GR/nm\ h^{-1})$ *and showed that P needs to be smaller than about 50 for a notable NPF to take place. However, it was noted that NPF occurred frequently in megacities in China where the calculated P values were much higher. They hypothesized that this discrepancy may be explained if the molecular clusters were being scavenged less effectively than expected based on their collision rates with pre-existing particles or if they grew much faster in size than our current understanding allows".*

In Section 3.8, we estimate the value of P from our results and compare it with the value predicted by Kulmala et al. (2017) for NPF. We have inserted the following text on page 18, lines 442-444:

"Our values of CS and GR give a cluster survival parameter P = 12 (Kulmala et al, 2017). This value is significantly lower than the maximum value of 50 that was specified as a condition for NPF."

Comment 3

Also, it could be interesting to compare the results here with those in Yu et al. (2016). Therein, they report in particle formation and growth rates during NPF events in Nanjing, also down to sub-3nm sizes.

Response 3

We agree. We have included the formation rate and growth rate values found by Yu et al. (2016) in Nanjing by inserting the following text at the end of section 3.7(Page 18, lines 425-429):

"These values may be compared with that found by Yu et al. (2016) in the urban atmosphere of Nanjing, China. They studied eight NPF events using a nano-condensation nucleus counter system capable of measuring particle size distributions down to 1.4 nm and estimated initial and peak particle formation rates of 210 and 2500 cm^{-3} s^{-1}, respectively. The formation rates showed good linear correlation with a sulfuric acid proxy".

And at the end of Section 3.8 (Page 18, lines 441-442):

"Yu et al. (2016) reported an exceptionally high local maximum growth rate of 25 nm h^{-1} in Nanjing, China.

Comment 4

Lines 277 & Fig. 3, line 287:
"Haze days" seems to be used interchangeably with "no-NPF days". Are they? If so, that point should be made clearer. If not, it may be feasible to mark them in Fig. 3. The various types of day are actually defined later on (lines 325-329). I suggest moving this definition to an earlier place, and then shortly mention it again later.

Response 4

In the original Figure 3, the NPF days were shown as red full markers. The points shown in white hollow markers were all other days, including normal (no-NPF) and haze days. We have changed the figure caption to read "other days" instead of "No-NPF Days".

Also, as suggested, we have moved the definition to the methods section and shortly mention it again at this point. The added text in Section 2.3.1 now reads as follows (Page 8, lines 184-188):

"A day on which there was at least one NPF event as defined above was termed an "NPF day". A day where the above criteria were not fulfilled were classified as a "non-event" day. A "haze day" was defined as a day when the 24-hour average $PM_{2.5}$ concentration exceeded 75 µg m^{-3} - the national air quality standard in China. A day on which there was neither NPF or haze was defined as a "normal day".

Comment 5

Line 318: "attachment to existing particles"

Response 5
This sentence was removed when the discussion on cluster concentrations was excluded.

Comment 6

I would have expected this process be more pronounced on the *no*-NPF days, when condensation sinks were higher.

Response 6

This statement was also removed when the discussion on cluster concentrations was excluded. However, we calculated the condensation sinks for no-NPF days and found that it was 0.006 s^{-1}, which is not significantly higher than the corresponding value on NPF days (0.005 s^{-1}). However, the condensation sink on haze days was 0.060 s^{-1}, which is significantly higher than both normal days and NPF days. We have inserted the following text into the end of section 3.6 on condensation sinks (Page 17, lines 404-408):

"The value of the condensation sink during NPF events (0.004 s^{-1}) was not significantly different to the corresponding average values during other times on NPF days and on normal days with no NPF (0.006 s^{-1}). However, the mean condensation sink on haze days (0.060 s^{-1}) was significantly higher than both these values."

Comment 7

Line 378: "previous have not been able"
I assume the authors refer to their novel measurement of particles in the 2-3 nm allowing them to more accurately calculating the coagulation sink (CoagS) for particles down to 2 nm. That's technically OK, but one would expect those small particles (i.e. in the 2-3 nm range for instance) to play a minor (negligible?) role in determining CoagS. How much is the value obtained here improved (increased) by the possibility to take the 2-3 nm range into account?

Response 7

Equation (5) for the formation rate considers the particles in the size range 2-3 nm. The rate of change of the number of particles in this size range was not available to previous workers. We use this, together with the coagulation sink of the particles in the size range 2-3 nm ($CoagSd_p$) to calculate the formation rate. The coagulation rate CoagS refers to the entire particle size range and this value is, as the reviewer points out, much larger than $CoagSd_p$ in the size range 2-3 nm. However, we thank the reviewer for this comment as it shows that the text was not very clear. We have modified the text as follows to make this as clear as possible:

In Section 2.3.3 (Page 11, lines 254-255) as follows:

"$CoagS_{dp}$ represents the loss of the particles due to coagulation in the size range 2-3 nm, calculated from equation (4) with d_p = 2 nm, and GR is the growth rate of particles".

And, in Section 3.7 (Page 17, lines 412-417):

"Using our value of the CS, we calculated the mean value of the coagulation sink using equation (4) for 2 nm particles during an NPF event to be 7.2x10^{-4} s^{-1}. Previous studies in Beijing have not been able to determine this value at 2 nm. The value reported for 3 nm particles for NPF events in Beijing by Wu et al. (2011) was 9.9x10^{-4} s^{-1}, which is close to our value at 2 nm. Using our value of the coagulation sink in equation (5), we calculated the formation rate of particles in the smallest particle size bin 2-3 nm".

Minor comments:

Comment 8

Abstract, 2nd sentence: The statement should be clarified. From what are the estimated characteristics different in the case of restricted measurements?

Response 8

We have modified this sentence as follows (Abstract, lines 30-32):

"Estimated characteristics of NPF events, such as their starting times and formation and growth rates of particles, are more accurate when the detection range of particles extends to smaller sizes."

Comment 9

Lines 152-153: It may be interesting and instructive for the reader to hear, in short, about the nature of the problems encountered.

Response 9

We have replaced this sentence with the following (Page 7, lines 169-170):

"Data was lost on nine days owing to various problems such as the loss of power, software malfunction and a blocked filter during a haze event."

Comment 10

Line 263: Does this t-test result apply to the whole measurement campaign, or just the subset shown in Fig. 2? In the latter case, would it change when applied to the whole period?

Response 10

This was for the subset shown in Fig 2. However, when we consider the entire monitoring period, the corresponding difference was even more significant. We have added the following sentence: (Page 13, lines 303-305)

"The corresponding difference was even more significant when considering the entire monitoring period where the mean daily values of $PM_{2.5}$ on NPF days and the other days were 21 $\mu g\ m^{-3}$ and 143 $\mu g\ m^{-3}$, respectively."

Comment 11

Line 297: "are more likely …" than what else?

Response 11

We have amended the text as follows on page 14, lines 338-431:
"Thus, the observed haze events are unlikely to be caused by in-situ new particle formation and more likely to be due to particles carried by the wind into the city or being prevented from escaping due to temperature inversions in the atmosphere".

Comment 12

Lines 329-332, Table 2: The source of the uncertainty of 20% has remained unclear to me. Maybe the authors can rephrase.

Response 12

We agree that the statement is unclear. We have replaced it with the following text on page 15, lines 361-364:

"The values shown are the means of the average $PM_{2.5}$ concentrations over all the 24-hour days. The daily mean values varied from day to day, especially on days with NPF events or haze events mainly due to the different durations of these events. We estimated the standard deviation about these mean values to be 20%".

Comment 13

Most figures have a gray background and odd dark-gray or blank frames. They would look better without any that.

Response 13

We have removed the grey background and frames around all figures.

Comment 14

The text/numbers in the color bar in Figures 2 and 7 are difficult to read and lack units.

Response 14

We have improved the quality of the numbers on the color bars and included units (cm^{-3}).

References:

Asmi, E., Sipilä, M., Manninen, H., Vanhanen, J., Lehtipalo, K., Gagné, S., Neitola, K., Mirme, A., Mirme, S., and Tamm, E.: Results of the first air ion spectrometer calibration and intercomparison workshop, Atmospheric Chemistry and Physics, 9, 141-154, 2009.
Brus, D., Skrabalova, L., Herrmann, E., Olenius, T., Travnickova, T., and Merikanto, J.: Temperature-dependent diffusion coefficient of H2SO4 in air: laboratory measurements using laminar flow technique, Atmos. Chem. Phys. Discuss., 2016, 1-26, 10.5194/acp-2016-398, 2016.
Curtius, J.: Nucleation of atmospheric aerosol particles, Comptes Rendus Physique, 7, 1027-1045, 2006.
Eisele, F., and Hanson, D.: First measurement of prenucleation molecular clusters, The Journal of Physical Chemistry A, 104, 830-836, 2000.
Guo, S., Hu, M., Zamora, M. L., Peng, J., Shang, D., Zheng, J., Du, Z., Wu, Z., Shao, M., and Zeng, L.: Elucidating severe urban haze formation in China, Proceedings of the National Academy of Sciences, 111, 17373-17378, 2014.
Jeong, K.: Condensation of water vapor and sulfuric acid in boiler flue gas, ProQuest, 2009.
Kulmala, M., Kerminen, V.-M., Petäjä, T., Aijun, D., and Wang, L.: Atmospheric Gas-to-Particle Conversion: why NPF events are observed in megacities?, Faraday Discussions, 2017.
Lugg, G.: Diffusion coefficients of some organic and other vapors in air, Analytical Chemistry, 40, 1072-1077, 1968.
Manninen, H., Franchin, A., Schobesberger, S., Hirsikko, A., Hakala, J., Skromulis, A., Kangasluoma, J., Ehn, M., Junninen, H., and Mirme, A.: Characterisation of corona-generated ions used in a Neutral cluster and Air Ion Spectrometer (NAIS), Atmospheric Measurement Techniques, 4, 2767, 2011.
Manninen, H. E., Mirme, S., Mirme, A., Petäjä, T., and Kulmala, M.: How to reliably detect molecular clusters and nucleation mode particles with Neutral cluster and Air Ion Spectrometer (NAIS), Atmos. Meas. Tech. Discuss, 2016.
Tang, M. J., Shiraiwa, M., Pöschl, U., Cox, R. A., and Kalberer, M.: Compilation and evaluation of gas phase diffusion coefficients of reactive trace gases in the atmosphere: Volume 2. Diffusivities of organic compounds, pressure-normalised mean free paths, and average Knudsen numbers for gas uptake calculations, Atmos. Chem. Phys., 15, 5585-5598, 10.5194/acp-15-5585-2015, 2015.
Williams, J.: Organic trace gases in the atmosphere: an overview, Environ. Chem., 1, 125-136, 2004.
Wu, Z., Hu, M., Liu, S., Wehner, B., Bauer, S., Wiedensohler, A., Petäjä, T., Dal Maso, M., and Kulmala, M.: New particle formation in Beijing, China: Statistical analysis of a 1-year data set, Journal of Geophysical Research: Atmospheres, 112, 2007.
Wu, Z., Hu, M., Yue, D., Wehner, B., and Wiedensohler, A.: Evolution of particle number size distribution in an urban atmosphere during episodes of heavy pollution and new particle formation, Science China Earth Sciences, 54, 1772, 2011.
Yu, H., Zhou, L., Dai, L., Shen, W., Dai, W., Zheng, J., Ma, Y., and Chen, M.: Nucleation and growth of sub-3 nm particles in the polluted urban atmosphere of a megacity in China, Atmospheric Chemistry and Physics, 16, 2641-2657, 2016.
Yue, D., Hu, M., Zhang, R., Wang, Z., Zheng, J., Wu, Z., Wiedensohler, A., He, L., Huang, X., and Zhu, T.: The roles of sulfuric acid in new particle formation and growth in the mega-city of Beijing, Atmospheric Chemistry and Physics, 10, 4953-4960, 2010.

Observations of Particles at their Formation Sizes in Beijing, China

Rohan Jayaratne[1†], Buddhi Pushpawela[1†], Congrong He[1], ~~Jian Gao[2],~~ Hui Li ~~Hui~~[2], Jian Gao[2*], Fahe Chai[2], Lidia Morawska[1*],

1 International Laboratory for Air Quality and Health, Queensland University of Technology, GPO Box 2434, Brisbane 4001, Australia.
2 Chinese Research Academy of Environmental Sciences, Beijing 100012, China.

Revised and Submitted to

Atmospheric Chemistry and Physics

~~February~~ May 2017

† Joint first authors.

* Joint c~~C~~orresponding author contact details:

Lidia Morawska

Tel: (617) 3138 2616; Fax: (617) 3138 9079

Email: l.morawska@qut.edu.au

Jian Gao

Formatted: Font: Not Bold

Tel: 010 84933433; Fax: 010 84915163

Email: gaojian@craes.org.cn

Abstract

New particle formation (NPF) has been observed in many highly polluted environments of South-East Asia, including Beijing, where the extent of its contribution to intense haze events is still an open question. Estimated characteristics of NPF events, such as their starting times and formation and growth rates of particles, are ~~very different when the measurements are restricted to particles in larger size ranges~~more accurate when the detection range of particles extends to smaller sizes. In order to understand the very first steps of particle formation, we used a neutral cluster and air ion spectrometer (NAIS) to investigate particle characteristics at sizes exactly where atmospheric nucleation and cluster activity occurs. Observations over a continuous three-month period in Beijing showed 26 NPF events. These events generally coincided with periods with relatively clean air when the wind direction was from the less-industrialized north. No NPF were observed when the daily mean $PM_{2.5}$ concentration exceeded 43 μg m^{-3}, which was the upper threshold for particle formation in Beijing. The fraction of particles that are charged in the size range 2-42 nm was normally about 15%. However, this fraction increased to 20-30% during haze events and decreased to below 10% during NPF events. With the NAIS, we determined the starting times of NPF very precisely to a greater accuracy than has been possible in Beijing before and provided a temporal distribution of NPF events with a maximum at about 8.30 am. Particle formation rates varied between ~~10-36~~12-38 cm^{-3} s^{-1}. Particle growth rates were estimated to be in the range 0.5-9.0 nm h^{-1}. These results are more reliable than previous studies in Beijing as the measurements were conducted for the first time at the exact sizes where clusters form into particles and provide useful insight into the formation of haze events.

Keywords: New particle formation, secondary particles, nucleation, haze events

1. Introduction

Particles in the atmosphere may be classified into two types depending on their origin. Primary particles are directly emitted by a source while secondary particles are formed through a secondary process by the homogeneous condensation of gaseous precursors. This is known as new particle formation (NPF) and has been observed in many parts of the world in many different types of environments (Curtius, 2006;Kulmala et al., 2005;Kulmala et al., 2004;Zhang et al., 2011). NPF is a complicated process where molecular clusters come together to form particles at a size of about 1.6 nm (Kulmala et al., 2004). Generally, it is favoured by clean air conditions where the particle number concentration (PNC) in the atmosphere is low, resulting in a lower particle surface available for the condensation of gases, leading to an increase of the supersaturation in the air enhancing homogeneous condensation of the gaseous species (Kulmala et al., 2005;Wu et al., 2011) and, therefore, NPF is less frequent in polluted environments. However, if the gaseous precursor concentration is high enough, NPF may occur at even higher particle concentrations (Kulmala et al., 2005;Wu et al., 2011). Jayaratne et al. (2015) showed that in the relatively clean environment of Brisbane, Australia, NPF do not occur when the ambient PM_{10} concentration exceeds about 20 μg m^{-3}. However, NPF have been commonly observed in more polluted environments like Beijing (Kulmama et al., 2016) and Shanghai (Xiao et al., 2015) in China. Kulmala et al (2017) proposed that the survival efficiency of clusters to form particles is determined by the two key parameters – condensation sink (CS) and cluster growth rate (GR). They defined a dimensionless survival parameter, P, equal to the ratio ($CS/10^{-4}$ s^{-1})/(GR/nm h^{-1}) and showed that P needs to be smaller than about 50 for a notable NPF to take place. However, it was noted that NPF occurred frequently in megacities in China where the calculated P values were much higher. They hypothesized that this discrepancy may be explained if the molecular clusters were being scavenged less effectively than

expected based on their collision rates with pre-existing particles or if they grew much faster in size than our current understanding allows.

The study of the formation and characteristics of NPF events in Beijing is important because of its possible influence on severe haze episodes (Guo et al., 2014;Huang et al., 2014). Such haze events not only give rise to poor visibility but are responsible for sharp increases in respiratory problems amongst the large population that is exposed. In particular, Beijing experienced severe haze episodes during November and December, 2015. Daily maximum $PM_{2.5}$ values in the city exceeded 500 µg m^{-3} on no less than six days during the month of December, prompting two official air pollution 'red alerts' to be issued (Xue et al., 2016). Close examination of the haze events demonstrate that they occur in cycles of a few days and generally coincide with winds blowing from the more polluted regions south of the city (Guo et al., 2014;Wu et al., 2007). Particulate matter concentrations are observed to drop significantly when the winds change to a northerly direction, bringing cleaner air into the city, which is when NPF events generally occur (Guo et al., 2014).

The earliest study of NPF using a TSI scanning mobility particle sizer (SMPS) in Beijing was carried out by Wehner et al. (2004). ~~They observed NPF on 25 out of 45 days of measurement with PNCs exceeding 10^5 cm^{-3}.~~ They observed NPF on 25 out of 45 days of measurement, and on each of these days the PNC exceeded 10^5 cm^{-3}. Subsequent studies using the SMPS were carried out by Wu et al. (2007) who showed that NPFs were observed on 50%, 20%, 35% and 45% of days during the spring, summer, fall and winter seasons, respectively. Yue et al. (2010) investigated 12 NPF events and showed that sulphuric acid and ammonia accounted for about 45% of the growth rate, with the balance being due to organic species. Guo et al. (2014) conducted a detailed analysis over a two-month period during the fall of 2013 and showed that NPF events occurred in a clear periodic cycle of about 4-7 days coinciding with northerly winds bringing cleaner air into the city. The average $PM_{2.5}$ values when the wind was from the north and when it was from the south were 35 and 114 µg

Formatted: Font: Not Italic

m^{-3}, respectively. The average $PM_{2.5}$ (and PNC) values during and outside the NPF periods were less than 50 µg m^{-3} (greater than 2 x 10^5 cm^{-3}) and several hundred µg m^{-3} (5 x 10^4 cm^{-3}), respectively. Pollution also originates from within the city – from motor vehicle emissions and industrial sources. In general, airborne gaseous pollutants in Beijing and other urban regions in China are mainly volatile organic compounds (VOC) and oxides of nitrogen (NO_x) from local transportation and sulphur dioxide (SO_2) from regional industrial sources (Wang et al., 2009;Yue et al., 2010). However, Guo et al. (2014) showed that the nucleation and growth processes occurred on a regional scale, over several hundred km, with the effect of local sources such as motor vehicle emissions being insignificant. A good summary of the studies conducted since 2004 in Beijing may be found in Zhibin et al. (2013) and Kulmama et al. (2016).

All these previous studies in Beijing have been carried out using the SMPS. The SMPS is a good tool to determine the PNC and size distribution down to a minimum particle size of about 3 nm, although the efficiency of detection falls off below about 10 nm. Thus, an event where aerosols in the size range 3-10 nm emitted on-site as primary particles or entrained from a distant location that continue to grow to larger sizes may be mistaken for particle formation at that monitoring site. The SMPS is also not able to identify the exact time period during which particle formation occurs. An instrument that can detect particles at smaller sizes is the neutral cluster and air ion spectrometer (NAIS) from Airel Ltd. The NAIS is specifically designed to monitor ~~particle formation~~NPF as it can detect particles down to ~~a size of 0.8 nm~~their actual formation sizes (Manninen et al., 2016;Manninen et al., 2009;Mirme et al., 2007). In this paper, we present the first results of using a NAIS in Beijing over the course of three months, two months with intense haze and very few NPF events, and the other including several days with NPF. We will investigate the characteristics of the NPF events and the conditions that gave rise to them. As the measurements included the sizes at which particles formed, the results provide more reliable information of such parameters as the starting times, growth rates and formation rates of particles than has been possible in the past.

2. Methods

2.1 Instrumentation

The NAIS is an improved version of the air ion spectrometer (AIS) which was developed by Airel Ltd (Mirme et al., 2007). In both instruments, the sample air is split equally into each of two separate cylindrical spectrometer columns, one of each polarity. At the inlet to each column, a unipolar corona wire diffusion charger of the same polarity as the central electrode in the column brings the particles to an equilibrium charge distribution. They are then classified by a differential mobility analyser where the outer electrodes consist of 21 insulated sections or rings, each with its own electrometer. The charged particles in the air flow are repelled by the central electrode which has a tapered cross-section and collected by the rings. The electric field between the central electrode and the rings is fixed by the voltage on the inner electrode and the gap between the inner and outer electrodes so that only particles in a given mobility range may be collected by each ring. In this way, the instrument can separate particles into 21 mobility or size bins. A refinement in the NAIS over the AIS is that it uses controlled charging to measure the concentration of charged particles in addition to the total PNC in each size range. This is done by switching the voltage off on the corona charger during one part of the measurement cycle. Thus, the NAIS can measure both charged and neutral particles separately. The mobility range of the instrument is 3.16-0.001 $cm^2 V^{-1} s^{-1}$ which corresponds to a mobility diameter range of 0.8-42 nm. However, Asmi et al. (2009), Manninen et al. (2011) and Manninen et al. (2016) have pointed out that the lowest detection limit for the NAIS in the particle mode is about 2.0 nm owing to the presence of corona-generated ions; at sizes smaller than 2.0 nm, the NAIS cannot reliably distinguish between charged and neutral particles, Therefore, Manninen et al. (2011) specified the lowest detection limit of the NAIS to be 1.6 and 1.7 nm for negative and positive ions, respectively, and 2.0 nm for neutral particles. Therefore, in this study, we will restrict our observations to the particle size range

Formatted: Font: Not Italic
Formatted: Font: Not Italic
Formatted: Font: Not Italic
Formatted: Font: Not Italic
Formatted: Font: Not Italic
Formatted: Font: Not Italic
Formatted: Font: Not Italic
Formatted: Font: Not Italic
Formatted: Font: Not Italic
Formatted: Font: Not Italic

2.0-42 nm. A good description of the detailed operation of the NAIS may be found in Manninen et al. (2016). In this study, we set the NAIS to a measurement cycle of 5 min consisting of 2 min each for charged and neutral particles with an offset period of 1 min. Thus, a PNC and charged particle concentration reading were obtained in real time once every 5 min.

The larger size PNC was monitored with an SMPS. The instrument was set to scan up and retrace times of 120 and 15 s respectively. The aerosol and sheath flow rates were 0.3 and 3.0 lpm, respectively. Size distributions were determined in 107 bins in the size range 14 to 673 nm. A complete size distribution record was obtained every 5 min. $PM_{2.5}$ concentrations were monitored with a tapered element oscillating monitor (TEOM) and recorded as hourly average values.

2.2 Study Design

The NAIS and SMPS were set up within a room on the roof of the Chinese Research in Atmospheric and Environmental Sciences (CRAES) Building in Beiyuan, Beijing, on the 28 October 2015 and monitoring was conducted continuously until 31 January 2016. This comprised 96 days including several episodes of very high pollution or haze days when the $PM_{2.5}$ in Beijing exceeded 100-200 μg m^{-3}. Data was lost on nine days owing to various problems such as the loss of power, software malfunction and a blocked filter during a haze event. ~~Owing to the high PM content in the air, the instrument experienced some problems on 9 days during which data was lost.~~ Air was sampled through a straight steel pipe of diameter 4 cm protruding vertically through the roof of the building. Meteorological parameters, including the wind speed, wind direction, air temperature and relative humidity were monitored and recorded hourly over the course of the study period.

~~2.2~~2.3 Analysis

~~2.2.1~~2.3.1 Identification of NPF events

The NAIS provided spectragrams showing the neutral and charged particle number size distributions in real time with the concentrations shown in colour contours. The neutral and charged PNCs were also provided in real time at 5 min intervals. NPF events were identified using the method proposed by Zhang et al. (2004). We calculated the rate of change of PNC, dN/dt, where N is the number of particles in the size range ~~1.8~~2.0 -10.0 nm. Events with N > 10,000 cm^{-3} for at least 1 hour and dN/dt >15,000 $cm^{-3}h^{-1}$ were classified as NPF events. These events generally exhibited a 'banana shape' in the spectragrams. A day on which there was at least one NPF event as defined above was termed an "NPF day". A day where the above criteria were not fulfilled were classified as a "non-event" day. A "haze day" was defined as a day when the 24-hour average $PM_{2.5}$ concentration exceeded 75 μg m^{-3} - the national air quality standard in China. A day on which there was neither NPF or haze was defined as a "normal day". NPF events are characterised by sharp increases in the intermediate size range. The starting times of an event was determined by using the time of sudden increase in PNC in the size range ~~1.8~~2.0 – 10.0 nm.

~~2.2.2~~2.3.2 Condensation sink (CS) and coagulation sink (CoagS)

The condensation sink of particles is defined as (Dal Maso et al., 2002;Dal Maso et al., 2005;Kulmala et al., 2012;Lehtinen et al., 2003;Salma et al., 2011)

$$CS = 2\,\pi\,D\,\sum_i \beta_m\,(d_{p,i}) d_{p,i} N_i \quad (1)$$

where D is the diffusion coefficient of the condensing vapour and β_m is the transition correction factor for mass flux. d_{pi} and N_i are the diameter and the number concentration of particles in the size bin i respectively. The unit of CS is s^{-1}.

It is now well established that sulfuric acid is the key precursor gas in nucleation, although low vapour pressure organics may contribute to the subsequent aerosol growth (Curtius, 2006). Sulfuric acid has a low vapour pressure which is reduced further in the presence of water. When produced from SO_2 in the gas phase, it is easily supersaturated and begins to condense. Moreover, most of the particles in the atmosphere are in the kinetic regime (smaller than 0.01 μm)(Seinfeld and Pandis, 2006). In this regime, condensation is directly proportional to the RMS speed of the molecules. The RMS speed is inversely proportional to the square root of the molecular weight of the molecule. Thus, a sulfuric acid molecule, with a molecular weight of 98 g mol^{-1}, has an RMS speed that is about 30% higher than a typical organic gas molecule with a molecular weight of about 200 g mol^{-1}, Thus, condensation of sulfuric acid will occur much more readily than organic molecules. Studies in Beijing have confirmed that NPF is more likely to occur in a sulfur-rich environment than in one that is sulfur-poor ((Yue et al., 2010;Guo et al., 2014;Wu et al., 2007)). Wu et al. (2007) also assumed that sulfuric acid was the main condensable vapour in determining the particle formation rates during NPF events in Beijing.

Therefore, a~~A~~ssuming that the main condensing vapour is sulphuric acid, we estimated the diffusion coefficient for condensing vapour using the expression

$$D = 5.0032 * 10^{-6} + 1.04 * 10^{-8} T + 1.64 * 10^{-11} T^2 - 1.566 * 10^{-14} T^3 \quad (2)$$

where D has the units of $m^2\ s^{-1}$ and where the temperature T is in Kelvin (Jeong, 2009).

The transition correction factor, β_m, was calculated using the Fuchs-Sutugin expression (Fuchs and Sutugin, 1971)

$$\beta_m = \frac{Kn + 1}{1 + (\frac{4}{3\alpha} + 0.337)Kn + (\frac{4}{3\alpha})Kn^2}$$

(3)

where

$$Kn = \frac{2\lambda}{d_p} \quad \text{and} \quad 0 \leq \alpha \leq 1 .$$

Here, *Kn*, the Knudsen number, describes the nature of the suspending vapour relative to the particle, λ is the mean free path of a suspending vapour molecule and d_p is the diameter of the particle (Seinfeld and Pandis, 2006). The mass accommodation coefficient (sticking coefficient) α describes the probability of a vapour molecule sticking to the surface of a particle during vapour-particle interactions (Seinfeld and Pandis, 2006). In this study, we assumed α = 1.

The relationship between the condensation sink and coagulation sink is given by Lehtinen et al. (2007) as

$$CoagS_{d_p} = CS.\left(\frac{d_p}{0.71}\right)^m$$

(4)

where the exponent m varies in the range -1.75 to -1.5 with a mean value -1.7 and the value 0.71 is the diameter of a hydrated sulphuric acid molecule. The unit of CoagS is s^{-1}.

In order to calculate the CS, we used the PNC obtained from the SMPS in the 107 size bins in the range 14-673 nm and from the NAIS in 8 size bins in the range 2-14 nm. The mean temperature in Beijing during the period of observation was close to 0°C. ~~We~~ The value of D calculated ~~D~~ using equation (2) at temperature T = ~~303~~ 273 K was 0.087 $cm^2 s^{-1}$ which is in good agreement with the values given in the literature (Brus et al. (2016), Eisele and Hanson (2000). ~~.~~ The values used for the exponent m was -1.7 (Dal Maso et al., 2008) and λ =108 nm (Massman, 1998).

~~2.2.3~~2.3.3 Particle formation rate

Particle formation or nucleation occurs from thermodynamically stable clusters in the size range 1.0-2.0 nm (Kulmala et al., 2007). The formation rate may be estimated from the number of particles in the smallest size bin, usually 2-3 nm in the NAIS.

The formation rate of particles is defined as

$$J_{d_p} = \frac{dN_{d_p}}{dt} + CoagS_{d_p}.N_{d_p} + \left(\frac{GR}{\Delta d_p}\right)N_{d_p} \quad (5)$$

where N_{dp} is the number concentration of particles in the size range d_p and ($d_p + \Delta d_p$) respectively (Kulmala et al., 2012). In this study, we used the values $d_p = 2$ nm and $\Delta d_p = 1$ nm, corresponding to the size range 2-3 nm. $CoagS_{dp}$ represents the loss of the particles due to coagulation in the size range 2-3 nm, calculated from equation (4) with $d_p = 2$ nm, and *GR* is the growth rate of particles. The unit of formation rate is $cm^{-3}\ s^{-1}$.

~~2.2.4~~2.2.4 Particle growth rate (GR)

During an NPF event, the growth rate of particles was defined by Kulmala et al. (2012) as

$$GR = \frac{dd_p}{dt} = \frac{d_{p2} - d_{p1}}{t_2 - t_1} \quad (6)$$

where dp_2 and dp_1 are the diameters of particles at times t_2 and t_1, respectively. This was calculated by the maximum concentration method as described in Kulmala et al. (2012) by examining the time of maximum PNC at each particle size during an NPF event. First, we exported the number concentrations of particles obtained from the NAIS in ~~15~~14 bins in the size range ~~1.8~~2.0 – 42.0 nm.

Next, we selected the time of maximum concentrations during each NPF event for each particle size bin. Finally, we calculated the growth rate using the slope of the best-fitted line on the graph of median diameter of particle in each size bin vs. the time of maximum concentration. The unit of GR is nm h^{-1}.

3. Results and Discussion

3.1 Distribution of NPF events

During the entire period of measurement, the NAIS yielded 87 complete days of data, the remaining 9 days being affected by instrument faults, generally due to power fluctuations. November and December 2015 were particularly prone to high pollution events in Beijing. The daily average $PM_{2.5}$ concentration exceeded the recommended maximum of 50 μg m^{-3} in Beijing on 47 days during this two-month period. The maximum daily average was 448 μg m^{-3} and this occurred on 1st December. Owing to the high condensation sink on polluted days, there were relatively few NPF days during these two months. There was a relative improvement of air quality after 4th January and this lasted until 31st January - the end of the monitoring period, during which time, the daily average exceeded 100 μg m^{-3} on only four days. Enhanced $PM_{2.5}$ concentrations (> 50 μg m^{-3}) were observed on 15 days in January. These days occurred in groups and we could identify five such distinct periods during January. No NPF events were observed during these 15 days; however, several NPF events were observed on the other days during the intervening periods. A summary of the observational days, together with the number of days on which data were available and NPF events were observed, are shown in Table 1. Column 3 shows the numbers of days on which complete 24-hour data were obtained. We note that, during the 56 such days between 27th October and 31st December, NPF events were observed on just 10 days, whereas during the 31 days in January 2016, NPF events took place on 16 days. The near equal division between NPF days and no-NPF days in January provided an ideal

data set to compare the parameters and conditions on these two types of days. The difference between November/December and January had a clear dependence on the $PM_{2.5}$ concentrations. Figure 1 gives a summary of the days on which NPF events were observed.

3.2 Relationship between NPF events and $PM_{2.5}$ concentration

In Fig 2, we take a closer look at the January data, together with the respective mean daily $PM_{2.5}$ concentrations. It is apparent that there were five distinct groups of NPF days in January. These are labelled in 2(b). In the NAIS spectragram, shown in 2(a), the 16 NPF events are clearly observed with the characteristic 'banana' shapes compressed into near-vertical bands extending up from the smallest sizes. The five groups from left to right consist of 5, 3, 2, 5 and 1 NPF events, respectively (Figs 2(a and b)). These groups are separated by time periods when no NPFs were observed. The $PM_{2.5}$ values are clearly lower on NPF days than on the other days with mean daily values of 18 μg m^{-3} and 120 μg m^{-3}, respectively. A Student's t-test showed that the difference in mean daily $PM_{2.5}$ values between NPF days and the other days was statistically significant at the confidence level of 95%. The corresponding difference was even more significant when considering the entire monitoring period where the mean daily values of $PM_{2.5}$ on NPF days and the other days were 21 μg m^{-3} and 143 μg m^{-3}, respectively. Figure 2(c) shows the corresponding mean daily PNC. While the PNC within each group showed a greater fluctuation than the $PM_{2.5}$, the PNC on NPF days was significantly higher than on non-NPF days. Therefore, although the PM is higher on haze days than on NPF days, the t-tests again showed that the PNC was significantly lower on haze days than on NPF days. This is explicable in terms of the particle size. Particles are significantly larger on haze days than on clean days when NPF events are likely to occur.

In Fig 3, we plot the daily mean PNC against the daily mean $PM_{2.5}$ for the 31 days in January. The days with NPF and the days with no NPF events clearly fall into two distinct groups according to

Formatted: Font: +Body (Calibri), Not Italic

Formatted: Indent: Left: 0.63 cm, Line spacing: Double, Adjust space between Latin and Asian text, Adjust space between Asian text and numbers

Formatted: Subscript

the daily mean $PM_{2.5}$ values. Pre-existing particles entering the region with the winds from the south will also increase the condensation sink, further reducing the likelihood of NPF.

No NPF events were observed on a day when the mean $PM_{2.5}$ value exceeded 43 µg m^{-3}. There is some minor overlap in the PNC values on the two types of days but this is primarily because they are daily averages. When we consider the average PNC values during the NPF events alone, a t-test showed that they are significantly higher than at other days and times. However, we do see that, on haze days, the daily average PNC does not exceed 8.5 x 10^4 cm^{-3}.

3.3 Relationship between NPF events and wind direction

Previous studies have shown that the wind direction played an important role in determining the $PM_{2.5}$ concentration in Beijing (Guo et al., 2014). Again, we look at the month of January, as it provided an almost equal number of NPF days and ~~non-NPF~~other days and was, therefore, ideal to compare the wind direction on the two types of days. Figure 4 shows the wind direction roses for both NPF days and ~~non-NPF~~other days during January. The frequencies are given as percentages of time when the wind was from a given direction. There is a clear difference between the two sets of days with a strong correlation between the NPF days and the wind direction. NPF events clearly occurred on days when the wind direction was predominantly from the NW, while it was more equally distributed with a greater likelihood of arriving from the S and E during the haze days when there were no NPF events. The frequencies in the sector between NW (315°) and N (0°) on NPF days and ~~non-NPF~~other days were 68 % and 11 %, respectively. Air from the north of Beijing is usually cleaner than that from the more industrialized south of the city (Guo et al., 2014). Clean periods are characterised by decreased condensation sinks that promote NPF. Winds from the south bring a copious supply of freshly available gaseous precursors that should give rise to particle formation. However, the absence of NPF events during these times suggests that the wind is also carrying a large supply of particles that reduce the gaseous supersaturations required for particle formation. Thus, the observed haze events are unlikely to be caused by in-situ new particle formation and more

Formatted: Subscript

Formatted: Font: (Default) +Body (Calibri), 11 pt, Not Italic, Font color: Auto

likely to be due to particles carried by the wind into the city or being prevented from escaping due to temperature inversions in the atmosphere~~Thus, the observed haze events are more likely to be due to particles carried by the wind into the city or being prevented from escaping due to temperature inversions in the atmosphere~~.

3.4 Charged particles ~~and clusters~~

Next, we look at the behaviour of ~~charged clusters and~~ charged particles, with particular attention to NPF events and haze events. In order to compare and contrast the characteristics of these particles, we selected a period of four days, comprising two haze days that were immediately followed by two NPF days. Figure 5 shows the time series of the concentration of total and charged particles ~~(a) and clusters (b)~~ observed over this four-day period from November 30 to December 3. ~~In Fig 5(a), t~~The upper curve represents the total PNC while the lower curve gives the charged PNC. The difference between the two curves gives the neutral PNC. ~~This is similar for the cluster concentrations in Fig 5(b).~~ The conditions during the two types of events could be compared during this period as intense haze was observed on the first two days (Nov 30 and Dec 1) while, following a change of wind direction near midnight on the 1 December, two strong NPF events took place on the next two days (Dec 2 and 3). ~~In general, the neutral cluster concentration exceeded the cluster ion concentration by about two orders of magnitude, with this ratio being somewhat greater when there was no particle formation. Large pools of neutral clusters were always observed to be present in previous studies in the boreal forests of Hyytiala, Finland (Kulmala et al., 2007) and in the urban environment of Brisbane, Australia (Jayaratne et al., 2016). Here, we can confirm the same observation in the more polluted Beijing atmosphere. The total cluster concentration showed a significant decrease, by almost an order of magnitude, as we passed from the first two days to the two NPF days. We attribute this to two phenomena – the attachment of clusters to existing particles and the conversion of clusters to new particles. We also see that less than 10% of the particles were charged, both during NPF days and when there were no NPF events.~~

A summary of the neutral and charged PNC ~~and cluster concentrations~~ during the various stages over the entire period of observation are presented in Table 2. Also shown are the percentage numbers of all particles that were found to be charged. NPF events and NPF days are defined in section ~~2.2.1~~2.3.1. A haze day was defined as a day when the 24-hour average $PM_{2.5}$ concentration exceeded 75 µg m^{-3} - the national air quality standard in China. A day that met neither of these criteria was defined as a 'normal day'. Thus, by our ad-hoc definition, a normal day had a daily average $PM_{2.5}$ concentration in the range 43-75 µg m^{-3}, since no NPF events were observed on days when the average $PM_{2.5}$ concentration was greater than 43 µg m^{-3}. The duration of the various events affected the daily values while the conditions during the events affected their peak number concentrations. The values shown are the means of the average $PM_{2.5}$ concentrations over all the 24-hour days. The daily mean values varied from day to day, especially on days with NPF events or haze events mainly due to the different durations of these events. We estimated the standard deviation about these mean values to be 20%~~This introduced an inherent uncertainty of up to 20% in the values shown in the table~~.

Formatted: Subscript

~~We note that only a very small percentage of clusters, less than 1%, are charged under all conditions.~~ On a normal day, around 15% of the particles larger than 2 nm are charged. The fraction that is charged decreases significantly during an NPF event. This is consistent with our observations in Brisbane (Jayaratne et al., 2016) and may be attributed to the rapid increase in particle number and the associated coagulation. On the other hand, during a haze event, the percentage of particles charged increases to a value between 20% and 30%. These observations are consistent with the PNC and particle sizes and the equilibrium distribution of charge on particles. NPF are characterised by large numbers of small particles while the SMPS and TEOM show that haze events comprise much larger particles. The amount of charge that a particle can hold and the fraction of particles that are

charged in equilibrium both increase with particle size, so it is not unexpected to find that a larger percentage of particles are charged during the haze events.

3.5 Particle formation times

All except one of the 26 NPF events during the period of observation began between 7:30 am and 10:00 am. The mean time was 8:45 am. This result is in agreement with Wu et al. (2007) who, using an SMPS, reported that NPF events during clean air periods in November, December and January generally started between 7:00 am and 10:00 am. Figure 6 shows the temporal distribution of the start times of the NPF events, classified into 30 minute bins. The most likely time for an NPF event to begin was between 8:00 and 8:30 am. This time coincides with the morning rush hour traffic when the production rate of gaseous precursors is generally at a maximum. Sunrise in Beijing in December/January is at about 7.30 am.

Figure 7 shows the NAIS spectragram of the strong NPF event that occurred on 29th October 2015. The spectragram shows a clear banana profile which levels off at about 20 nm. The PNC in this event was relatively high, exceeding 1.6 x 10^5 cm^{-3} near 11:00 am. The $PM_{2.5}$ concentration remained between 12 and 16 µg m^{-3} right through this event. The markers shown on this figure are the median sizes of particles at each time. It can be observed ~~I~~in the spectragram~~, the transition time from clusters to particles, at around 2 nm, is very sharp and we can conclude that~~ that particle formation began at around 09:00 h. However, previous studies in Beijing have not been able to measure particles smaller than 3 nm. In Fig 7, if we truncate the lower particle size margin to 3 nm, the starting time of the NPF event appears later than it actually is, approximately at 9:30 am. In other NPF spectragrams, we see this difference being as much as 1.0 to 1.5 h depending on the initial growth rate. Thus, we conclude that the starting times that we have derived (Fig 6) are more accurate than has been obtained in the past. This will also affect the estimated growth rates of particles during NPF events as we shall show in the next section.

3.6 Condensation ~~and coagulation sinks~~sink

The condensation ~~and coagulation~~ sinks were calculated during NPF events assuming the growth to be due to sulfuric acid and using the SMPS and NAIS data and the equations given in the methods section. The mean value of the condensation sink was ~~5~~4.2x10^{-3} s^{-1}. This value is somewhat smaller than that reported by Wu et al. (2007) (1.4x10^{-2} s^{-1}) and Wu et al. (2011) (1x10^{-2} s^{-1}) but within the range of 0 – 5x10^{-2} s^{-1} reported in all NPF events between 2004 to 2008 in Beijing by Zhibin et al. (2013). ~~The mean value of our coagulation sink for 2 nm particles during an NPF event was 9x10^{-4} s^{-1}. Previous studies in Beijing have not been able to determine this value at 2 nm. The values reported for 3, 5 and 10 nm for NPF events in Beijing by Wu et al. (2011) are 9.9x10^{-4} s^{-1}, 4.3x10^{-4} s^{-1} and 1.4x10^{-4} s^{-1}, respectively. The value at 3 nm is close to our value at 2 nm.~~ The value of the condensation sink during NPF events (0.004 s^{-1}) was not significantly different to the corresponding average values during other times on NPF days and on normal days with no NPF (0.006 s^{-1}). However, the mean condensation sink on haze days (0.060 s^{-1}) was significantly higher than both these values.

3.7 Particle formation rate

Using ~~the values of the condensation and coagulation sinks in equation 5~~our value of the CS, we calculated the~~The~~ mean value of ~~our~~the coagulation sink using equation (4) for 2 nm particles during an NPF event ~~was~~to be ~~9~~7.2x10^{-4} s^{-1}. Previous studies in Beijing have not been able to determine this value at 2 nm. The value~~s~~ reported for 3~~, 5 and 10~~ nm particles for NPF events in Beijing by Wu et al. (2011) ~~are~~was 9.9x10^{-4} s^{-1}, ~~4.3x10^{-4} s^{-1} and 1.4x10^{-4} s^{-1}, respectively. The value at 3 nm~~which is close to our value at 2 nm. Using our value of the coagulation sink in equation (5), we calculated the

Formatted: Line spacing: Double

Formatted: Font: Not Italic

Formatted: Font: Not Italic

Formatted: Font: Not Italic

formation rate of particles in the smallest particle size bin 2-3 nm. At these times, ~~where~~ the rate of increase of particles in this size bin ranged from about 5.0×10^3 to 1.5×10^4 cm^{-3} h^{-1}. The resulting formation rates varied between ~~10~~ 12 and ~~36~~ 38 cm^{-3} s^{-1}, with a mean of ~~23~~ 26 cm^{-3} s^{-1}. Previous estimates in Beijing did not have the benefit of the PNC information in the 2-3 nm size bin. Wu et al. (2007) calculated the formation rate in the wider size bin of 3-10 nm and arrived at a value in the range 3.3-81.4 cm^{-3} s^{-1} with a mean of 22.3 cm^{-3} s^{-1}. Yue et al. (2010) studied 12 NPF events in Beijing and derived a formation rate in the range 2-13 cm^{-3} s^{-1} and showed that the formation rate was directly proportional to the sulfuric acid concentration. They did not specify the size range used in this calculation but the smallest detectable particle size of the instrument used was 3 nm. These values may be compared with that found by Yu et al. (2016) in the urban atmosphere of Nanjing, China. They studied eight NPF events using a nano-condensation nucleus counter system capable of measuring particle size distributions down to 1.4 nm and estimated initial and peak particle formation rates of 2.1×10^2 and 2.5×10^3 cm^{-3} s^{-1}, respectively. The formation rates showed good linear correlation with a sulfuric acid proxy.

Formatted: Font: +Body (Calibri), 11 pt, Not Italic

Formatted: Font: +Body (Calibri), 11 pt, Not Italic

Formatted: Font: +Body (Calibri), 11 pt, Not Italic

Formatted: Font: +Body (Calibri), 11 pt, Not Italic

3.8 Particle growth rate

In the NPF event shown in Fig 7, the particle growth rate in the size range 2-10 nm ~~soon after formation is about 9 nm h^{-1}. The average growth rate~~ during the entire event (between 9:00 and 11:00 am) estimated from equation (6) was 4.8 nm h^{-1}. Although the PNC reached very high values, the particles did not grow much larger than about 30 nm, suggesting that the high condensation sink was restricting the precursor gas concentration in the atmosphere. The growth rate of all the NPFs observed ranged from 0.5 to 9.0 nm h^{-1} with a mean value of 3.5 nm h^{-1}. Previous estimates of the growth rate during NPF using the SMPS have yielded mean values of 1.0 nm h^{-1} (Wehner et al., 2004) and 1.8 nm h^{-1} (Wu et al., 2007)., 2007). Zhibin et al. (2013) determined the growth rates of a number of NPFs in Beijing over a 4-year period and reported a range of 0.1 to 10 nm h^{-1} with a mean

of 3.0 nm h^{-1} which is in close agreement with our value. In contrast, Yu et al (2016) reported an exceptionally high local maximum growth rate of 25 nm h^{-1} in Nanjing, China. Our values of CS and GR give a cluster survival parameter P = 12 (Kulmala et al, 2017). This value is significantly lower than the maximum value of 50 that was specified as a condition for NPF.

4. Summary and Conclusions

We monitored charged and neutral PNC over a continuous three-month period for the first time in Beijing. The results showed 26 NPF events. No NPF were observed when the daily mean $PM_{2.5}$ concentration exceeded 43 μg m^{-3}.

A summary of the main parameters determined are shown in Table 3.

This is the first study of NPF in the particle size range below 3 nm in Beijing. This enables the derivation of more relevant and accurate estimates of parameters, such as the times of formation and growth and formation rates, than has been possible before.

The results show the following features of NPF events in Beijing:

- NPF events occur during clean air episodes when the wind direction is from the north of the city.
- We have provided the first temporal distribution chart of NPF events in Beijing which shows that all but one of the 26 events began between 7:30 and 10:00 am.
- The main characteristics of the particles in the NPF events are presented in Table 3.
- ~~In general, less than 10% of particles were charged and less than 1% of the clusters were charged.~~
- The fraction of particles that are charged was normally about 15%. This fraction increased to 20-30% during haze events and decreased to below 10% during NPF events.

Acknowledgements

This project was supported by the Australia-China Centre for Air Quality Science and Management., the National Natural Science Foundation of China (Grant No 41375132, 91544226), and the Special

Funds for Research on Public Welfares of the Ministry of Environmental Protection of China (201409003). We thank Zhipeng Bai and Wen Yang for their assistance with the project.

Formatted: Space After: 0 pt, Line spacing: Double

References

Curtius, J.: Nucleation of atmospheric aerosol particles, Comptes Rendus Physique, 7, 1027-1045, 2006.

Dal Maso, M., Kulmala, M., Lehtinen, K., Mäkelä, J., Aalto, P., and O'Dowd, C.: Condensation and coagulation sinks and formation of nucleation mode particles in coastal and boreal forest boundary layers, Journal of Geophysical Research: Atmospheres, 107, 2002.

Dal Maso, M., Kulmala, M., Riipinen, I., Wagner, R., Hussein, T., Aalto, P. P., and Lehtinen, K. E.: Formation and growth of fresh atmospheric aerosols: eight years of aerosol size distribution data from SMEAR II, Hyytiala, Finland, Boreal Environment Research, 10, 323, 2005.

Dal Maso, M., Hyvärinen, A., Komppula, M., Tunved, P., KERMINEN, V., Lihavainen, H., Viisanen, Y., HANSSON, H. C., and Kulmala, M.: Annual and interannual variation in boreal forest aerosol particle number and volume concentration and their connection to particle formation, Tellus B, 60, 495-508, 2008.

Fuchs, N., and Sutugin, A.: High-dispersed aerosols, Topics in Current Aerosol Research GM Hidy, JR Brock, 1–60, in, Pergamon, New York, 1971.

Guo, S., Hu, M., Zamora, M. L., Peng, J., Shang, D., Zheng, J., Du, Z., Wu, Z., Shao, M., and Zeng, L.: Elucidating severe urban haze formation in China, Proceedings of the National Academy of Sciences, 111, 17373-17378, 2014.

Huang, R.-J., Zhang, Y., Bozzetti, C., Ho, K.-F., Cao, J.-J., Han, Y., Daellenbach, K. R., Slowik, J. G., Platt, S. M., and Canonaco, F.: High secondary aerosol contribution to particulate pollution during haze events in China, Nature, 514, 218-222, 2014.

Jayaratne, E., Clifford, S., and Morawska, L.: Atmospheric Visibility and PM10 as Indicators of New Particle Formation in an Urban Environment, Environmental science & technology, 49, 12751-12757, 2015.

533 Jayaratne, E. R., Ling, X., and Morawska, L.: Charging State of Aerosols during Particle Formation
534 Events in an Urban Environment and Its Implications for Ion-Induced Nucleation, Aerosol and Air
535 Quality Research, 16, 348-360, 2016.
536 Jeong, K.: Condensation of water vapor and sulfuric acid in boiler flue gas, ProQuest, 2009.
537 Kulmala, M., Vehkamaki, H., Petaja, T., Dal Maso, M., Lauri, A., Kerminen, V., Birmilli, W., and
538 McMurry, P.: Formation and Growth Rates of Ultrafine Atmospheric Particles: A Review of
539 Observations, Journal of Aerosol Science, 35, 143-176, 2004.
540 Kulmala, M., Petäjä, T., Mönkkönen, P., Koponen, I., Maso, M. D., Aalto, P., Lehtinen, K., and
541 Kerminen, V.-M.: On the growth of nucleation mode particles: source rates of condensable vapor in
542 polluted and clean environments, Atmospheric Chemistry and Physics, 5, 409-416, 2005.
543 Kulmala, M., Riipinen, I., Sipilä, M., Manninen, H. E., Petäjä, T., Junninen, H., Dal Maso, M., Mordas,
544 G., Mirme, A., and Vana, M.: Toward direct measurement of atmospheric nucleation, Science, 318,
545 89-92, 2007.
546 Kulmala, M., Petäjä, T., Nieminen, T., Sipilä, M., Manninen, H. E., Lehtipalo, K., Dal Maso, M., Aalto,
547 P. P., Junninen, H., and Paasonen, P.: Measurement of the nucleation of atmospheric aerosol
548 particles, Nature protocols, 7, 1651-1667, 2012.
549 Kulmama, M., Petäjä, T., Kerminen, V.-M., Kujansuu, J., Ruuskanen, T., Ding, A., Nie, W., Hu, M.,
550 Wang, Z., and Wu, Z.: On secondary new particle formation in China, Frontiers of Environmental
551 Science & Engineering, 10, 1-10, 2016.
552 Lehtinen, K. E., Korhonen, H., Maso, M., and Kulmala, M.: On the concept of condensation sink
553 diameter, Boreal environment research, 8, 405-412, 2003.
554 Lehtinen, K. E., Dal Maso, M., Kulmala, M., and Kerminen, V.-M.: Estimating nucleation rates from
555 apparent particle formation rates and vice versa: Revised formulation of the Kerminen–Kulmala
556 equation, Journal of Aerosol Science, 38, 988-994, 2007.
557 Manninen, H. E., Petaja, T., Asmi, E., Ripinen, I., Nieminen, T., Mikkila, J., Horrak, U., Mirme, A.,
558 Mirme, S., Laakso, L., Kerminen, V., and Kulmala, M.: Long-term field measurements of charged and

559 neutral clusters using Neutral cluster and Air Ion Spectrometer (NAIS), Boreal Environment Research,
560 14, 591-605, 2009.
561 Manninen, H. E., Mirme, S., Mirme, A., Petäjä, T., and Kulmala, M.: How to reliably detect molecular
562 clusters and nucleation mode particles with Neutral cluster and Air Ion Spectrometer (NAIS), Atmos.
563 Meas. Tech. Discuss, 2016.
564 Massman, W.: A review of the molecular diffusivities of H 2 O, CO 2, CH 4, CO, O 3, SO 2, NH 3, N 2 O,
565 NO, and NO 2 in air, O 2 and N 2 near STP, Atmospheric Environment, 32, 1111-1127, 1998.
566 Mirme, A., Tamm, E., Mordas, G., Vana, M., Uin, J., Mirme, S., Bernotas, T., Laakso, L., Hirsikko, A.,
567 and Kulmala, M.: A wide-range multi-channel Air Ion Spectrometer, Boreal Environmental Research,
568 12, 247-264, 2007.
569 Salma, I., Borsós, T., Weidinger, T., Aalto, P., Hussein, T., Dal Maso, M., and Kulmala, M.: Production,
570 growth and properties of ultrafine atmospheric aerosol particles in an urban environment, Atmos.
571 Chem. Phys, 11, 1339-1353, 2011.
572 Seinfeld, J. H., and Pandis, S. N.: Atmospheric chemistry and physics. Hoboken, NJ: Wiley, 2006.
573 Wang, M., Zhu, T., Zheng, J., Zhang, R., Zhang, S., Xie, X., Han, Y., and Li, Y.: Use of a mobile
574 laboratory to evaluate changes in on-road air pollutants during the Beijing 2008 Summer Olympics,
575 Atmospheric Chemistry and Physics, 9, 8247-8263, 2009.
576 Wehner, B., Wiedensohler, A., Tuch, T., Wu, Z., Hu, M., Slanina, J., and Kiang, C.: Variability of the
577 aerosol number size distribution in Beijing, China: New particle formation, dust storms, and high
578 continental background, Geophysical Research Letters, 31, 2004.
579 Wu, Z., Hu, M., Liu, S., Wehner, B., Bauer, S., Wiedensohler, A., Petäjä, T., Dal Maso, M., and
580 Kulmala, M.: New particle formation in Beijing, China: Statistical analysis of a 1-year data set, Journal
581 of Geophysical Research: Atmospheres, 112, 2007.
582 Wu, Z., Hu, M., Yue, D., Wehner, B., and Wiedensohler, A.: Evolution of particle number size
583 distribution in an urban atmosphere during episodes of heavy pollution and new particle formation,
584 Science China Earth Sciences, 54, 1772-1778, 2011.

585 Xiao, S., Wang, M., Yao, L., Kulmala, M., Zhou, B., Yang, X., Chen, J., Wang, D., Fu, Q., and Worsnop,
586 D.: Strong atmospheric new particle formation in winter in urban Shanghai, China, Atmospheric
587 Chemistry and Physics, 15, 1769-1781, 2015.
588 Xue, Y., Zhou, Z., Nie, T., Pan, T., Qi, J., Nie, L., Wang, Z., Li, Y., Li, X., and Tian, H.: Exploring the
589 Severe Haze in Beijing During December, 2015: Pollution Process and Emissions Variation, Huan jing
590 ke xue= Huanjing kexue/[bian ji, Zhongguo ke xue yuan huan jing ke xue wei yuan hui" Huan jing ke
591 xue" bian ji wei yuan hui.], 37, 1593, 2016.
592 Yue, D., Hu, M., Zhang, R., Wang, Z., Zheng, J., Wu, Z., Wiedensohler, A., He, L., Huang, X., and Zhu,
593 T.: The roles of sulfuric acid in new particle formation and growth in the mega-city of Beijing,
594 Atmospheric Chemistry and Physics, 10, 4953-4960, 2010.
595 Zhang, Q., Stanier, C., Canagaratna, M., Jayne, J., Worsnop, D., Pandis, S., and Jiminez, J.: Insights
596 into the Chemistry of New Particle Formation and Growth Events in Pittsburgh Based on Aerosol
597 Mass Spectrometry, Environmental Science and Technology, 38, 4797-4809, 2004.
598 Zhang, R., Khalizov, A., Wang, L., Hu, M., and Xu, W.: Nucleation and growth of nanoparticles in the
599 atmosphere, Chemical Reviews, 112, 1957-2011, 2011.
600 Zhibin, W., Min, H., Zhijun, W., and Dingli, Y.: Reasearch on the Formation Mechanisms of New
601 Particles in the Atmosphere, Acta Chimica Sinica, 71, 519-527, 2013.

602

603

Figures

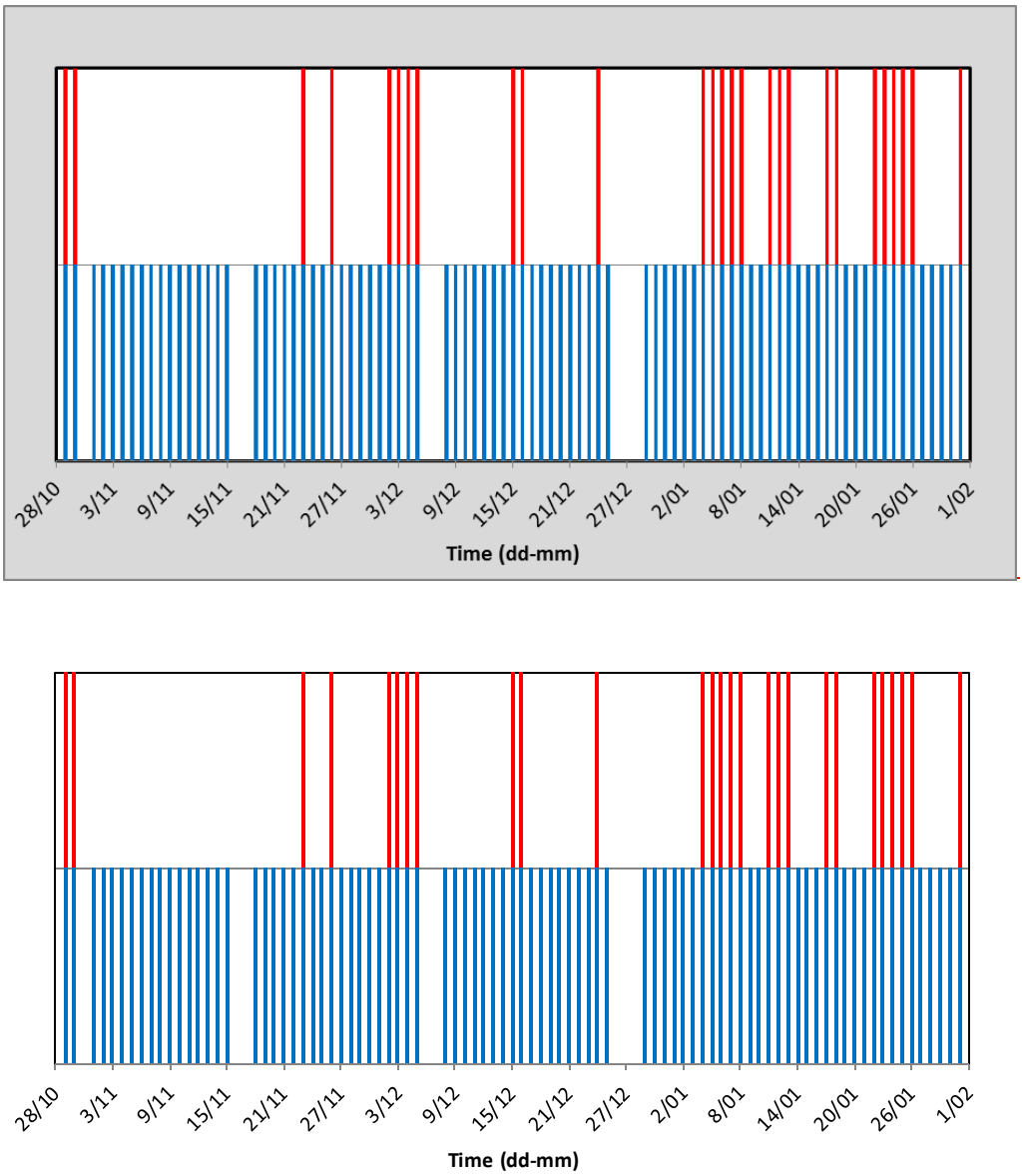

Figure 1: Summary of observational days (lower panel in blue) and days with NPF events (upper panel in red).

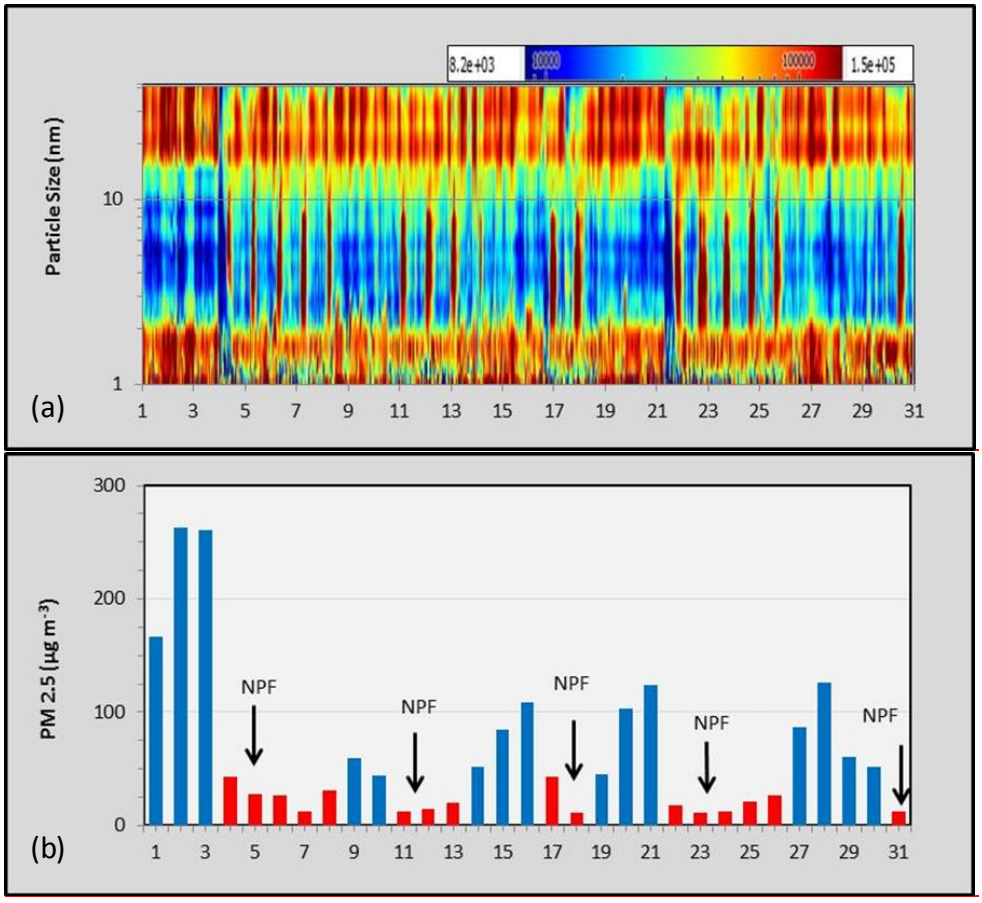
8.2e+03
1.5e+05
Particle Size (nm)
10
1
(a)
1 3 5 7 9 11 13 15 17 19 21 23 25 27 29 31
PM 2.5 (μg m-3)
300
200
100
0
NPF
NPF
NPF
NPF
NPF
(b)
1 3 5 7 9 11 13 15 17 19 21 23 25 27 29 31

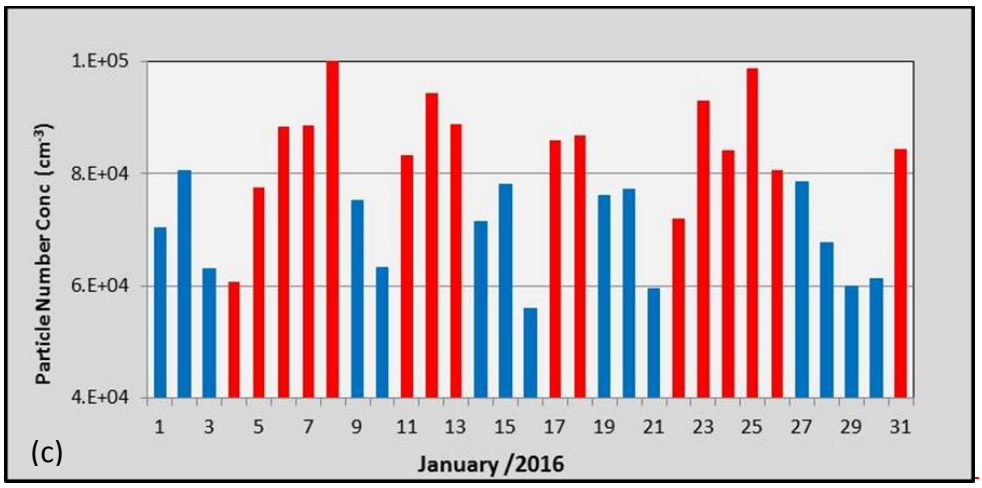
1.E+05
8.E+04
6.E+04
4.E+04
Particle Number Conc (cm-3)
1 3 5 7 9 11 13 15 17 19 21 23 25 27 29 31
January /2016
(c)

624

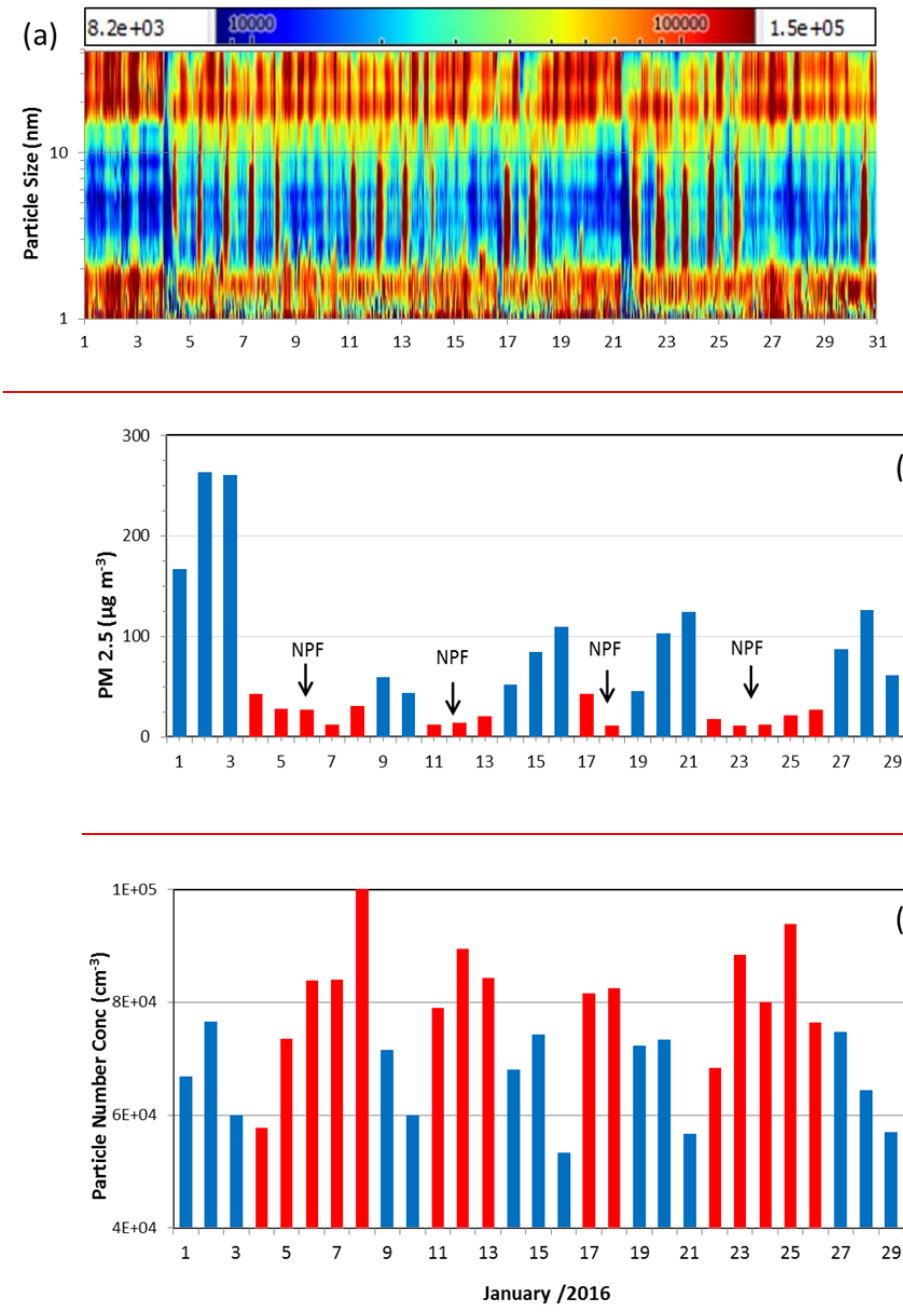

Figure 2: Daily values for January 2016: (a) NAIS Spectragram of PNC on a particle size–time diagram (b) mean $PM_{2.5}$ concentration from the TEOM and (c) mean PNC in the size range ~~1.8~~2 – 42 nm from the NAIS. In (a), the units of PNC are cm^{-3}. Data below 2.0 nm should be treated

with caution due to instrumentation limitations as described in the text. In (c), t~~T~~he red and blue bars represent the NPF days and ~~Non-NPF~~other days, respectively.

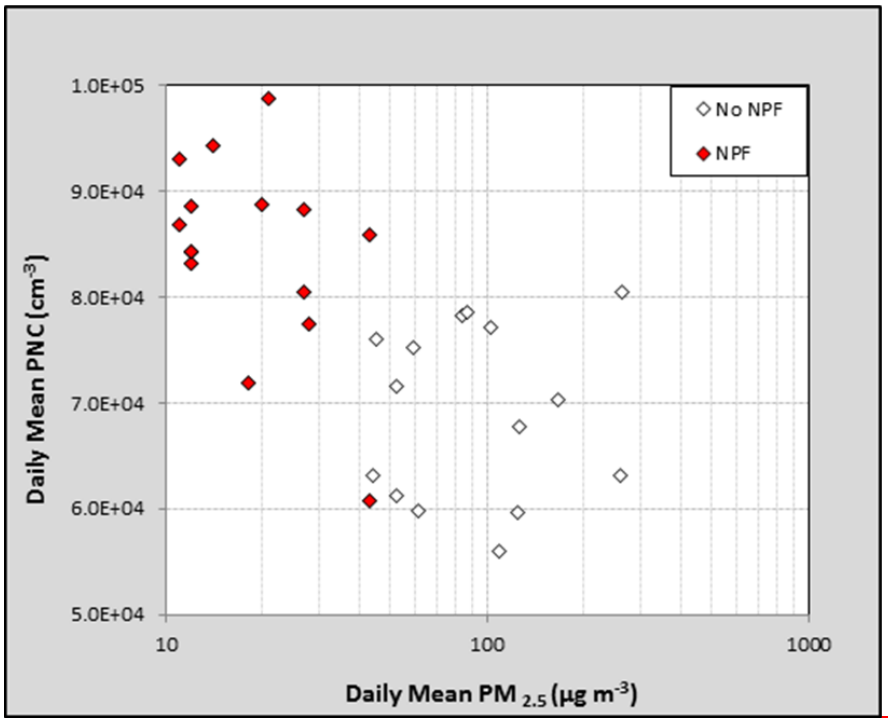

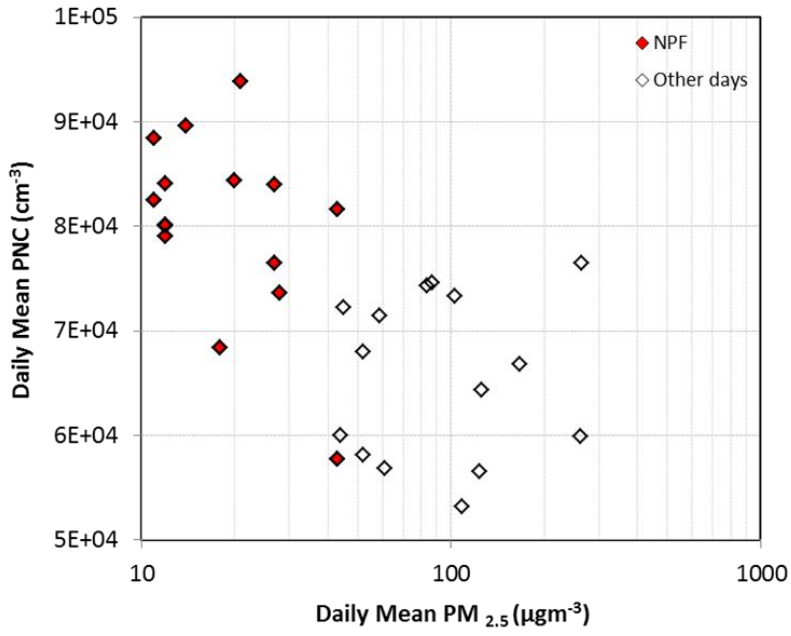

Figure 3: Daily mean PNC vs $PM_{2.5}$ for NPF days (filled markers) and ~~no NPF~~other days (open markers) during January 2016.

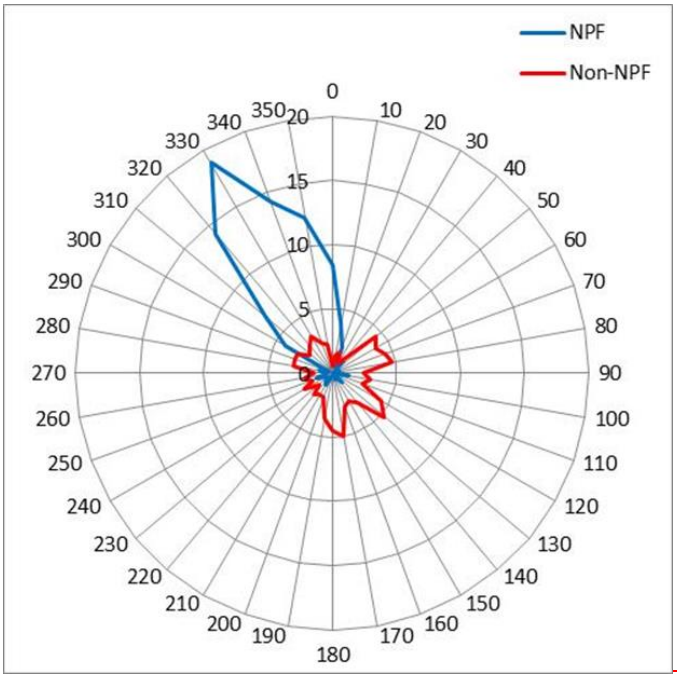

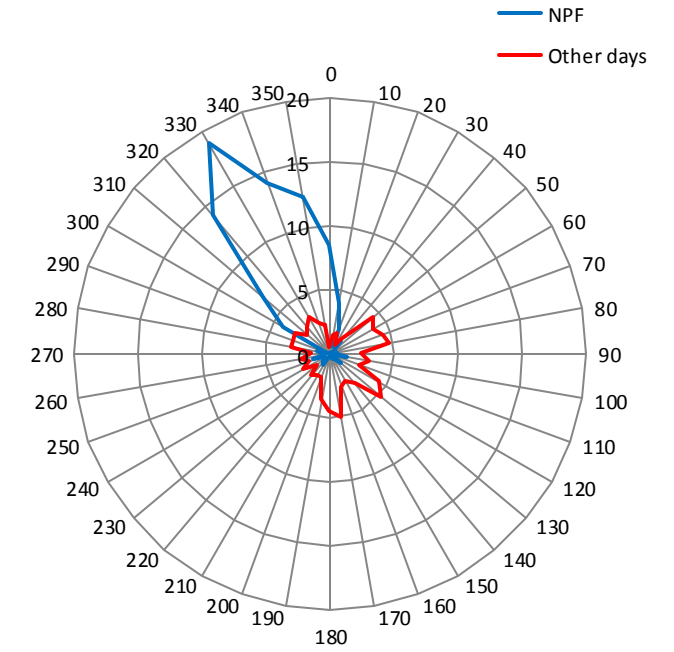

Figure 4: The wind direction rose for NPF days and ~~non-NPF~~other days during January. The radial scale indicates percentages of time.

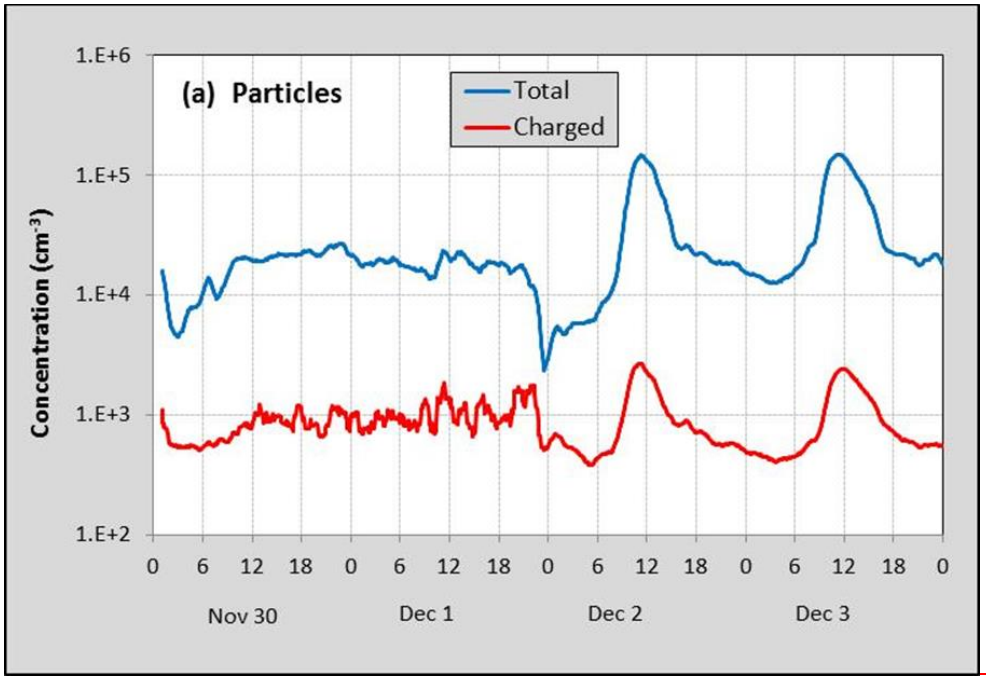
(a) Particles
Total
Charged
Concentration (cm-3)
1.E+6
1.E+5
1.E+4
1.E+3
1.E+2
0 6 12 18 0 6 12 18 0 6 12 18 0 6 12 18 0
Nov 30
Dec 1
Dec 2
Dec 3

655

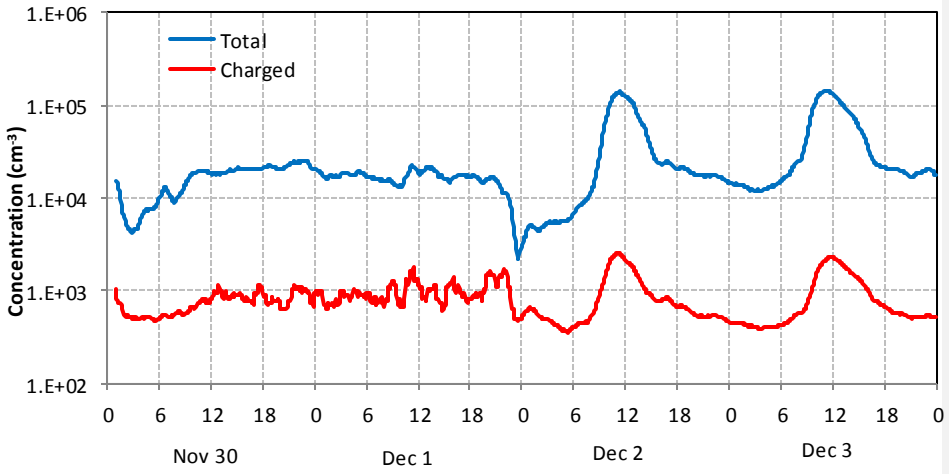
Total
Charged
Concentration (cm-3)
1.E+06
1.E+05
1.E+04
1.E+03
1.E+02
0 6 12 18 0 6 12 18 0 6 12 18 0 6 12 18 0
Nov 30
Dec 1
Dec 2
Dec 3

656

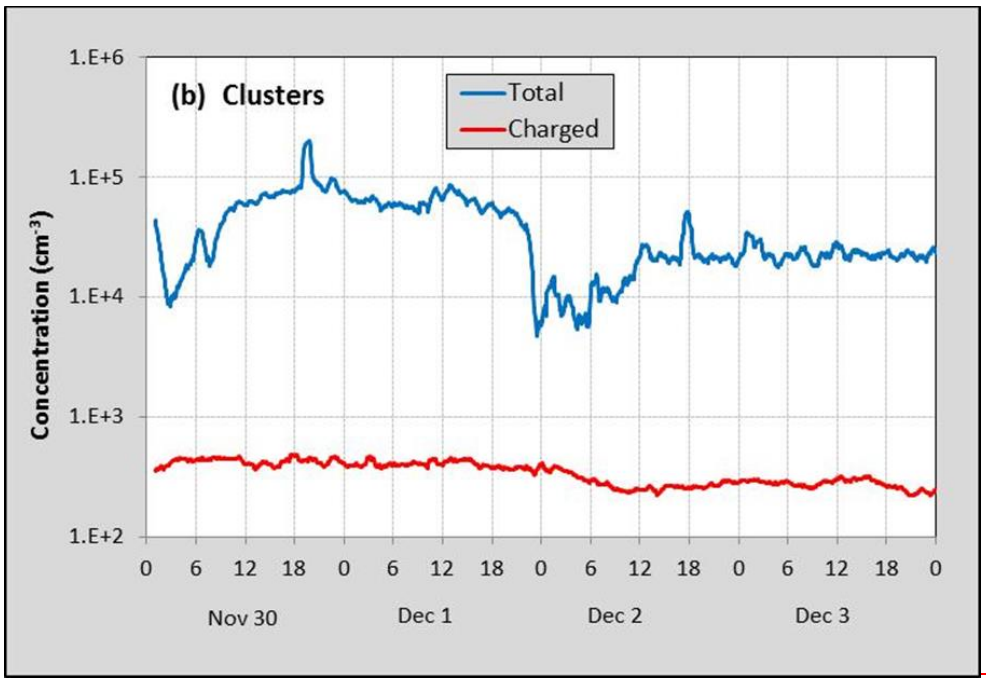

Figure 5: Time series of total and charged ~~(a)~~ particles ~~and (b) clusters~~ during the period 30 Nov to 3 Dec as measured by the NAIS. 30 Nov and 1 Dec were haze days while two NPF events occurred on 2 and 3 Dec.

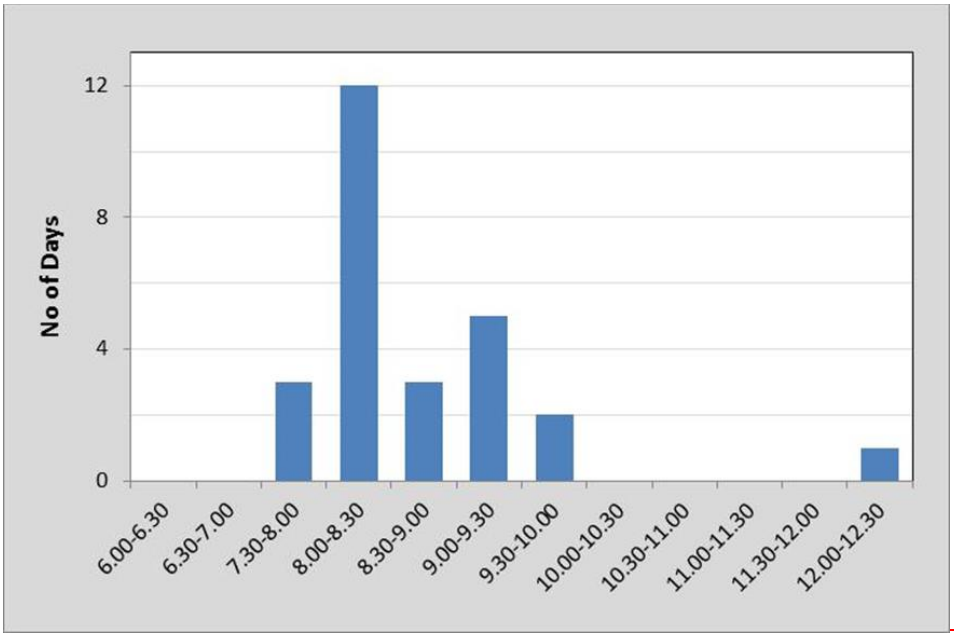

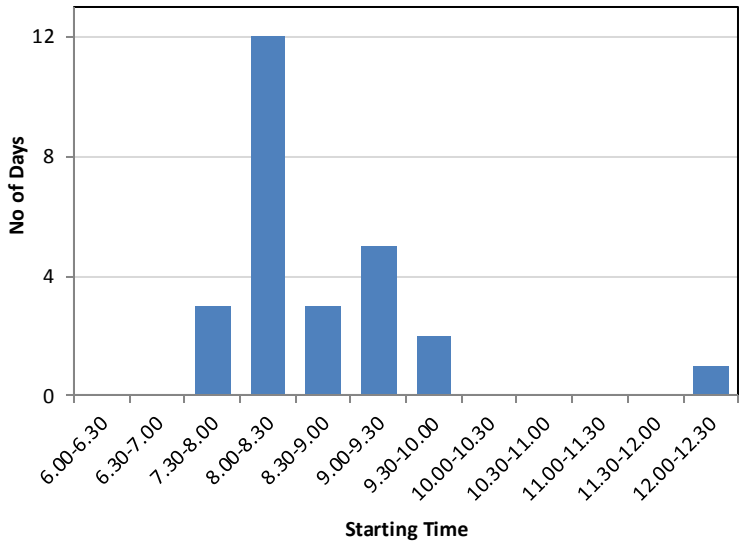

Figure 6: Distribution of the start times of the NPF events, classified into 30 min bins.

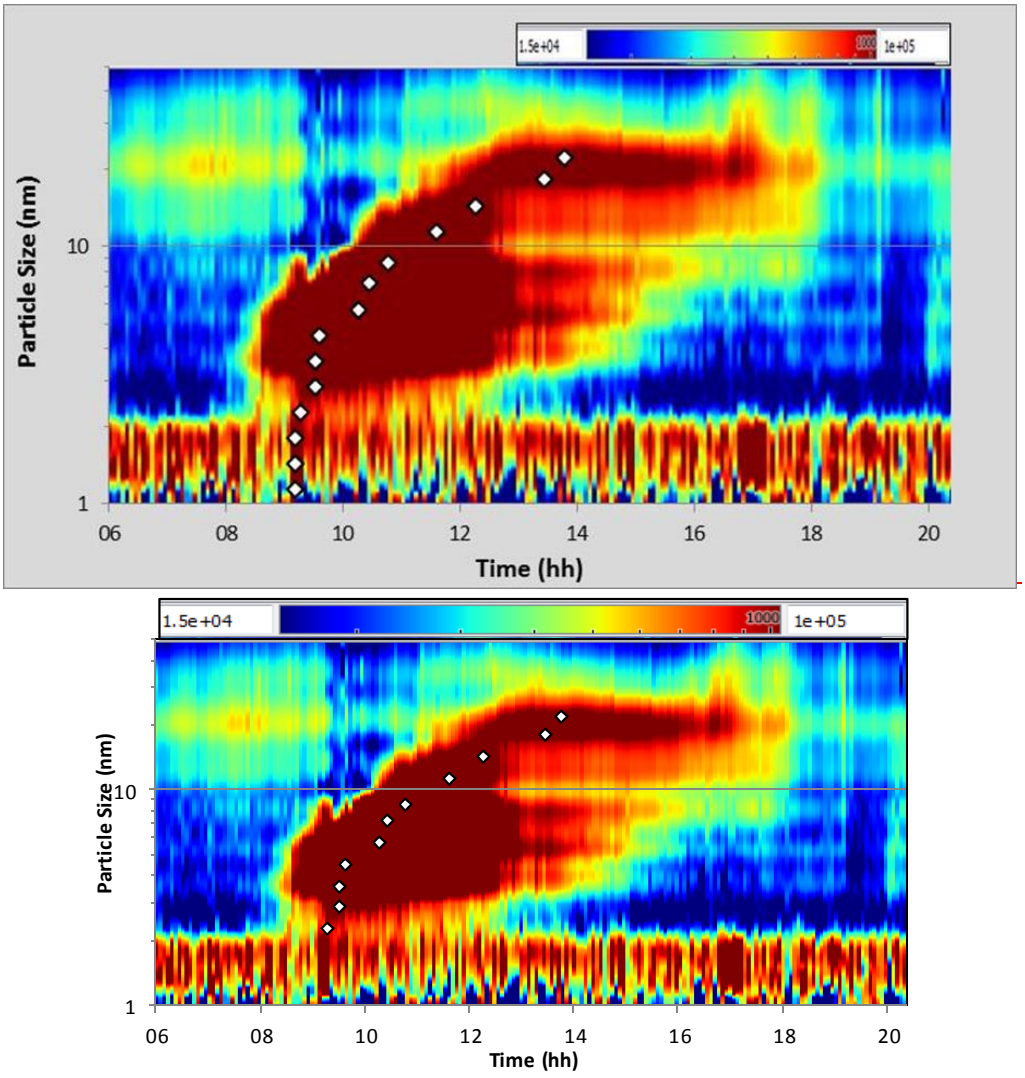

Figure 7: NAIS spectragram of the NPF event that occurred on 29th October. The clear banana shape indicates strong particle growth. The markers show the median particle size at each time. The units of PNC are cm^{-3}. Data below 2.0 nm should be treated with caution due to instrumentation limitations as described in the text.

679
680
681
682
683
684
685
686
687
688
689
690
691
692 **Tables**

693 Table 1: Summary of the observational days.

Month	Total Days	Data Available Days	NPF Days : dN/dt >15000 cm^{-3} h^{-1}
October (28-31)	4	2	2
November (1-30)	30	28	2
December (1-31)	31	26	6
January (1-31)	31	31	16
Total	96	87	26

694
695
696
697
698

Table 2: Mean and peak values of neutral and charged particle and cluster concentrations during the various types of days and events. The associated uncertainties in the values are up to 20%. The two % columns shows the respective charged/total percentages.

	Particles (cm^{-3})			Clusters (cm^{-3})		
	Neutral ($x10^4$)	Charged ($x10^4$)	%	Neutral ($x10^4$)	Charged ($x10^2$)	%
Normal Days (mean)	5.9	1.0	15.0	3.1	1.5	0.5
NPF Days (mean)	8.0	0.9	10.1	2.6	1.4	0.5
NPF Events (peak)	23.7	1.4	5.4	4.9	3.3	0.7
Haze Days (mean)	5.0	2.0	28.2	3.8	2.4	0.6
Haze Events (peak)	12.3	3.1	20.0	9.9	4.8	0.5

	Particles (cm^{-3})		
	Neutral ($x10^4$)	Charged ($x10^4$)	%
Normal Days (mean)	5.6	0.9	14.5
NPF Days (mean)	7.6	0.8	10.1
NPF Events (peak)	22.5	1.3	5.6
Haze Days (mean)	4.8	1.9	28.6
Haze Events (peak)	11.7	2.9	20.1

Table 3: Summary of mean and range of parameters calculated for the NPF events observed.

Parameter	Mean	Range
Starting Time of NPF	8.45 am	7.30 am – 12.30 pm
Condensation sink (s^{-1})	5×10^{-3}	$(2.1 - 8.9) \times 10^{-3}$
Coagulation sink (s^{-1})	9×10^{-4}	$(3.6 - 15.3) \times 10^{-4}$
Formation rate (J_2) ($cm^{-3} s^{-1}$)	23	10 – 36

~~Growth rate (nm h^{-1})~~ ~~3.5~~ ~~0.5 - 9.0~~

Parameter	Mean	Range
Starting Time of NPF	8.45 am	7.30 am - 12.30 pm
Condensation sink (s^{-1})	4.2 x 10^{-3}	(2.3 - 5.7) x 10^{-3}
Coagulation sink (s^{-1})	7.2 x 10^{-4}	(3.9 - 9.7) x 10^{-4}
Formation rate (J_2) (cm^{-3} s^{-1})	26	12 - 38
Growth rate (nm h^{-1})	3.5	0.5 - 9.0

732

733